RHENIUM COMPLEXES WITH O, N, S LIGANDS

A Thesis presented to the Faculty of the Graduate School
University of Missouri-Columbia

In Partial Fulfillment
Of the Requirements for the Degree

Master of Science

---

by
SULOCHANA JUNNOTULA

Dr. Silvia S. Jurisson, Thesis Supervisor

DECEMBER 2006

The undersigned appointed by the dean of the Graduate School, have examined the thesis entitled

RHENIUM COMPLEXES WITH O, N, S LIGANDS

Presented by Sulochana Junnotula,

a candidate for the degree of Master of Science

and hereby certify that in their opinion it is worthy of acceptance

Silvia Jurisson

J. David Robertson

Michael R. Lewis

……..To my grand mother, parents and husband

ACKNOWLEDGMENTS

First of all, I would like to thank Professor Silvia S. Jurisson, my advisor for her help, encouragement, guidance and support throughout my graduate study. I can feel her care and concern all the time. She was always there for me. It was a wonderful opportunity to work in her group.

I would like to thank Dr. Heather Bigott and Dr. Engelbrecht Hendrik for their help in my projects. Their mentorship helped me to learn many things in the lab.

I would like to acknowledge the Jurisson group. It is a very friendly atmosphere here. I would like to specially mention Stephanie Lane, Yongjian Liu and Beau Ballard.

I want to thank Dr. Michael R. Lewis for his consistent support and encouragement. His willingness to teach is always memorable. Special thanks to Dr. J. David Robertson for spending his valuable time on my defense.

I want to thank my grand mother Amrithamma for her love and affection. I am indebted to my parents Pushpa Latha and Raji Reddy for their encouragement, love and support. Without them I would have not made up to my graduate study. I want to specially mention my darling sister Manjula, she is the sweetest person, also I want to thank my brother and his family.

Last but not least, I want to thank the most important and adorable person in my life, my husband, Venkatraman Junnotula for being there for me, for encouraging, guiding and supporting whatever I do and for making my life easier.

TABLE OF CONTENTS

LIST OF FIGURES

Figure **Page**

LIST OF SCHEMES

Scheme **Page**

LIST OF TABLES

Table **Page**

Chapter 1

Introduction

1.1 History of Nuclear Medicine

More than 100 years ago, in November 1895, Wilhelm Conrad Roentgen discovered X-rays. Soon after this discovery, others began investigating the possibility that these mysterious rays might kill germs. Based on the work of Roentgen, Henri Becquerel discovered X-rays produced by Uranium in early 1896.[1] A few years later, Marie and Pierre Curie isolated and identified radium from uranium. Radium was used to cure many diseases in the early 1900s.[2] In 1935, Irene Curie and Frederic Joliot successfully produced artificial radionuclides, which led to the development of radiotracer studies by Georg de Hevesy and for which he received the Nobel Prize in Chemistry in 1943.[2]

The field of nuclear medicine was established following the application of the "radiotracer theory" proposed by Georg de Hevesy. Nuclear medicine can be defined as a specialty in medicine, which deals with the use of radiopharmaceuticals or radiotracers.

1.2 Considerations for Radiopharmaceuticals

Radiopharmaceuticals are radioactive compounds used for the diagnosis and treatment of diseases. More than 85% of radiopharmaceuticals are used for diagnostic purposes, while the rest are used for therapeutic applications.[6]

There are several aspects to consider while designing new radiopharmaceuticals. For example, the type of radionuclide, nuclear characteristics such as decay mechanism, half-life, production methods, etc., maintain an important role in the effectiveness of the agent.

The type of radionuclide plays an important role in preparing a radiopharmaceutical. Nuclear properties determine which radionuclides are useful, and for which application. In addition to the radionuclide selected, most radiopharmaceuticals have an additional component that binds or incorporates the radionuclide to form a radioactive complex. The mode of incorporation depends on the elemental chemistry of the radionuclide. Metallic elements require the formation of a coordination complex with the additional component, whereas nonmetallic elements are often directly incorporated into the compound through a covalent bond. The coordination number and the structural conformation of the coordination complex vary according to the elemental chemistry and the oxidation state of the metal.

An ideal radionuclide for a diagnostic agent emits a photon or gamma ray. Photons and gamma rays interact poorly with low atomic number elements such as carbon, nitrogen and oxygen found in the human body, so they escape out of the body and will be captured by gamma cameras.

An ideal radionuclide for therapy emits particles such as beta, alpha, conversion electrons or Auger electrons. Particles interact with DNA in the nucleus resulting in irreparable damage to the DNA strands, which ultimately inhibits cellular reproduction.

The half-life of the radionuclide should not be so long that it irradiates the normal organs for a long time, which would result in a high dose of radiation. It should not be so short that there is not sufficient time for synthesis of the radiopharmaceutical, shipping to hospitals, administration to patients, and either imaging or therapy studies. The method of production is important because the radionuclide should have high specific activity and high radionuclidic purity. The radionuclidic complex should be stable to dissociation

under biological conditions. It should also be resistant to chemical or electrochemical reactions in the body.

1.3 Diagnostic Radiopharmaceuticals

The application of X-rays on humans led to the birth of diagnostic imaging in medicine. Today, in addition to X-rays several other imaging modalities have been developed such as Computed Tomography (CT), Magnetic Resonance Imaging (MRI), Ultrasound, etc. By using these techniques, the structural changes that occur with tumor growth or various other diseases can be observed. Diagnostic radiopharmaceuticals allow physicians to see both anatomic as well as pathophysiologic processes of different organ systems of the human body. Physicians use different radiopharmaceuticals or radiotracer drugs to evaluate function of different organ systems, such as the kidneys, thyroid, ventricular function of the heart, myocardial or cerebral perfusion, etc. They also evaluate different disease states such as musculoskeletal diseases, primary and metastatic tumors, etc.

An ideal diagnostic radiopharmaceutical requires the use of a radionuclide whose emission penetrates out of the body for detection. As stated previously, the ideal radionuclide for imaging emits γ-rays or photons (X-rays or annihilation photons from positron emission). The emissions from these radionuclides are detected by NaI(Tl) detectors or bismuth germanium oxide (BGO) detectors.[3,4] The imaging is done by SPECT (Single Photon Emission Computed Tomography) and PET (Positron Emission Tomography), depending on the emission.

SPECT scanners detect the gamma rays and X-rays emitted from the radionuclide. ^{99m}Tc emits a single 141 keV gamma ray, which is suitable for imaging with SPECT.

^{99m}Tc-radiopharmaceuticals are currently being used for more than 85% of all diagnostic scans in hospitals.[5,6] The half life of ^{99m}Tc is 6 hours, which is ideal to prepare the drug, as well as to attain quality images of the patient.[7] Some of the ^{99m}Tc radiopharmaceuticals on the market are brain imaging agents such as technetium-99m-[*d,l*-hexamethylpropylene amine oxime] (^{99m}Tc-*d,l*-HM-PAO or Ceretec®) and technetium-99m-[N, N'-1, 2-ethylenediyl-bis-L-Cysteine diethyl ester) (^{99m}Tc-*l,l*-ECD or Neurolite®).[8,9] There are many other ^{99m}Tc-imaging agents available on the market.[3]

PET scanners detect the two 511 keV annihilation photons emitted when the positron interacts with an electron in matter. Some of the isotopes used for PET are F-18, O-15, Rb-82, C-11, etc. A current FDA approved PET radiopharmaceutical is ^{18}F-fluorodeoxyglucose (FDG).[10]

1.4 Therapeutic Radiopharmaceuticals

Therapeutic radiopharmaceuticals are radioactive compounds used to treat diseases. As described previously, ideal therapeutic agents contain a radioactive isotope that emits a particle, such as alpha, beta, Auger electron, etc.[6,8]

Alpha particles are high energy Helium nuclei. They are large in size and charge, and have high LET. Due to these reasons, they travel only small distances and cause the most ionizing damage over a small distance.

Beta particles are high energy electrons emitted from the nucleus. They have a much greater range than alpha particles but the low ionization density along their tracks accounts for their low LET properties.

Auger electrons are emitted during electron capture and internal conversion. Auger electrons deposit high amounts of energy over sub-cellular dimensions (decay site), resulting in more efficient killing of the tumor cells to which Auger emitters have localized.

There are several therapeutic radiopharmaceuticals available on the market for treating tumors. But compared with diagnostic radiopharmaceuticals, therapeutic radiopharmaceuticals are fewer in number. Some of the FDA approved therapeutic radiopharmaceuticals are ^{153}Sm-EDTMP for metastatic bone disease, ^{131}I-sodium iodide for treatment of thyroid disorders, and ^{90}Y-Zevalin® or I-131 Bexxar® for Non Hodgkins B-cell Lymphomas. [11-14]

1.5 Design of Radiopharmaceuticals

Although the purpose of the diagnostic and therapeutic radiopharmaceuticals is different, their design is similar. A large number of radiolabeling techniques have been developed.[15] Two of them are frequently used in producing metallic radiopharmaceuticals. One is the Bifunctional Chelate Approach (BFCA) and the other is the Integrated Approach.[6]

In the BFCA approach the radiometal is coordinated to a chelating agent, which is attached to the targeting moiety (Figure 1.1). Sometimes a linker may help in attaching the radiometal complex to the targeting moiety.

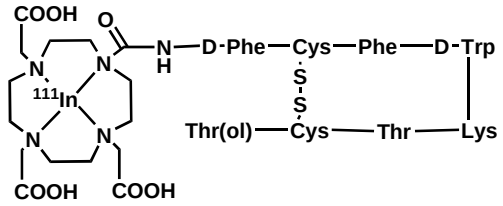

Figure 1.1: Bifunctional Chelate Approach

In the BFCA approach, the radiometal is not directly introduced into the targeting moiety, so it may not cause a disturbance in the binding structure and conformation of the targeting vector, and thus may not affect the affinity and uptake of the targeting vector to its receptor. But the chelating agent coordinated to the radioactive metal should satisfy the coordination sphere of the radiometal and should form a thermodynamically and kinetically inert complex. If the chelating agent does not form a stable radioactive metal complex, the radiometal may dissociate from the chelating agent after introduction of the radiopharmaceutical into the patient, which may result in unnecessary radiation doses to normal organs.

In some cases the radionuclide is directly incorporated into the targeting moiety. This approach in designing radiopharmaceuticals is called the integrated approach[15] (Figure 1.2).

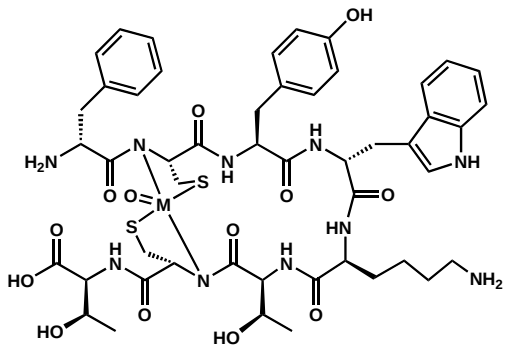

Figure 1.2: Integrated Approach

Introducing a radiometal directly into the targeting moiety may help in improving the stability of a radiopharmaceutical. It may also aid in improving the tumor uptake and retention. For example, the use of the integrated approach resulted in the greatest tumor uptake and retention observed for the Tc-99m and Re-188 labeled α-CCMSH analogues.[16] But sometimes the change in conformation produced by binding of the radiometal to the targeting agent may lead to a decrease in receptor binding. For example with the α-MSH analogues, Ac-Cys-Glu-His-D-Phe-Arg-Trp-Cys-Lys-Pro-Val-NH_2, direct metallation into the disulfide bond resulted in a cyclic structure with lower receptor binding than the disulfide cyclized analogues.[15] It turned out that the metal (Re or Tc) had coordinated to the two Cys sulfhydryls, a Trp amide, and the Trp nitrogen. Since the Trp is required for receptor binding, the metal coordination interfered with this process. An additional Cys residue was added to the N-terminus to yield CCMSH analogues, which resulted in second generation radiometallated derivatives with high specific receptor binding, high tumor uptake, and longer tumor residence times.[17]

1.6 Thesis Summary

The goal of this thesis is the synthesis, characterization and purification of Re-complexes containing O, N, S ligands. Chapter 2 describes the synthesis, purification and characterization of four Re-complexed somatostatin analogues, in which the integrated approach was used for designing the molecules. Chapter 3 describes the synthesis of three rhenium complexes, two of them with amine ligands and the third complex containing an amine thiol ligand. The Re-amine complexes were characterized by NMR, IR and mass spectroscopies. The pKa determinations of the amine complexes

were performed to determine the effect of the R groups on the amine N or the carbon back bone of the amine ligand.

References

1. Ehmann, William D.; Vance, Diane, Radiochemistry and Nuclear Methods of Analysis. **1991,** John Wiley & Sons, Inc.

2. Eugene. L. Saenger, and Gloria D. Adamek. Marie Curie and Nuclear Medicine: Closure of a Circle. *Med. Phys*. **1999,** 26, 1761-1765

3. Saha, G. Fundamentals of Nuclear Pharmacy 3rd ed. Springer-Verlag: New York, **1992**.

4. Wang, C.; Willis, D.; Loveland, W. Radiotracer Methodology in the Biological, Environmental and Physical Sciences. Prentice-Hall: New Jersey, **1975**.

5. Anderson C. J.; Welch, M. J. Radiometal-Labeled Agents (Non-Technetium) for Diagnostic imaging. *Chem Rev.* **1999,** 99, 2219-2234.

6. Jurisson, S. S.; Lydon J. D. "Potential Technitium Small Molecule Radiopharmaceuticals". *Chem Rev.* **1999,** 99, 2205-2218.

7. Jones, A.G. Technetium in Nuclear Medicine. *Radiochim*. *Acta.* **1995,** 70, 289-297.

8. Jurisson, S. S.; Berning, D.; Jia, W.; Ma, Dangshe. Coordination Cmpounds in Nuclear Medicine. *Chem Reviews.* **1993,** 93, 1137-1156.

9. Van Aswegen, A.; Roodt, A.; Marais, J.; Botha, J. M.; Naude, H.; Lotter, M.G.; Goedhals, L.; Doman, M. J.; Otto, A. C. Radiation Dose estimates of 186Re-hydroxo ethylidene diphosphonate for palliation of metastatic osseous lesions in animal study. N*ucl. Med. Comm.* **1997,** 18, 582-588.

10. Franzius, H. E.; Daldrup-Link.; J. Sciuk.; E. J. Rummerny.; S. Bielack.; H. Jurgens.; O. Schober. FDG-PET for detection of pulmonary metastases from malignant primary bone tumors. *Annals of Oncology.* **2001**, 12, 479-486

11. M. Farhanghi.; R. A. Holmes.; W. A. Volkert.; K. W. Logan and A. Singh. Samarium 153-EDTMP: Pharmacokinetic, toxicity and pain response using an escalating dose schedule in treatment of metastatic bone cancer. *J. Nuc. Med.* **1992,** 33, 1451-1458.

12. Herath, K. B. Gembicki, M.; Piyasena, R. D.; Wikramanayake, T. W. Thyroid scintiscanning using 131I-sodium iodide. A review of 150 scans. The *Ceylon Med J.* **1974**, 19, 160-164.

13. Cilley, Jeffrey.; Winter, Jane N. Radioimmunotherapy and autologous stem cell transplantation for the treatment of B-cell lymphomas. *Haematologica.* **2006**, 91, 114-120.

14. R. O. Dillman. Radioimmunotherapy of B-cell Lymphoma with Radiolabelled AntiCD20 monoclonal antibodies. *Clinical and Experimental Medicine*. 2006, 6, 1-12

15. Liu, S.; Edwards, D.S. Technetium Labeled Small Peptides as Diagnostic Radiopharmaceuticals. C*hem Rev.* **1999,** 99, 2235-2268.

16. Giblin, M. F.; Wang, N.; Jurisson, S. S. and Quinn, T. P. Synthesis and Characterization of rhenium complexed α-melanotropin analogs. *Bioconjugate Chem.* **1997**, *8*, 347-353.

17. Giblin, M. F.; Wang, N.; Hoffman, T. J.; Jurisson, S. S. and Quinn, T. P. Design and characterization of α-melanotropin peptide analogs cyclized through rhenium and technetium metal coordination. *Proc. Natl. Acad. Sci. U.S.A.* **1998,** 95, 12814-12818

CHAPTER 2

Rhenium-Cyclized Somatostatin Analogues

2.1 Introduction

Somatostatins are 14 amino acid and 28 amino acid cyclic peptides.[1] They appear in several organ systems such as the hypothalamopituitary system, gastrointestinal tract, pancreas, etc. They inhibit a wide spectrum of physiological functions including peptide hormone secretion.

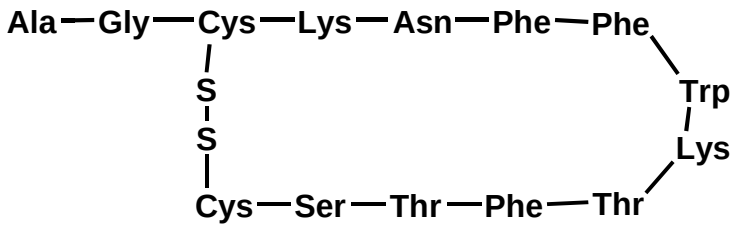

Figure 2.1: Somatostatin-14

Somatostatin receptors are molecular structures present on the surface of a cell that bind with somatostatin. There are five somatostatin receptors subtypes identified in different organs in the human body: Sst1, Sst2, Sst3, Sst4 and Sst5.[1] A high density of somatostatin receptors are expressed on majority of tumors such as growth hormone-secreting pituitary adenomas, gastroenteropancreatic tumors, phaeochromocytomas, etc. Most tumor tissues preferentially express Sst2 receptors, and less frequently express Sst1, Sst3 and Sst5. The Sst4 receptor is only rarely detected.

Somatostatins are degraded *in vivo* by peptidases, causing them to clear from the circulation very rapidly (2-3 min). To overcome this drawback, somatostatin analogues have been prepared. Octreotide, one of these analogues, contains D-amino acids and a *C*-

terminal alcohol group, and a disulfide bond between its two cysteine residues (Figure 3.2). It was originally developed as a chemotherapeutic agent.

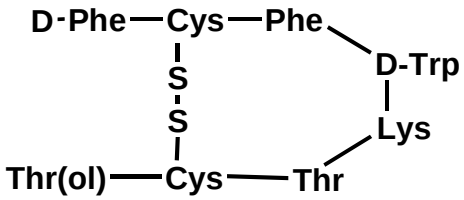

Figure 2.2: Octreotide

Researchers at the University of Rotterdam modified the basic octreotide by replacing phenylalanine with tyrosine at position 3.[2] The presence of tyrosine permits radiolabelling with ^{123}I or ^{131}I. ^{123}I emits 159 keV gamma which is useful for imaging. ^{131}I emit 364 keV gamma and 610 keV beta which are useful for both imaging and therapy respectively.[2] But the major limitation of the iodine labeled Tyr^3-octreotate was it's high uptake in non targeted organs like liver, stomach, pancreas, intestine etc. In addition to this ^{123}I is not readily available, difficult to label, deiodinates easily *in vivo* and has a low physiological half-life.

To overcome this difficulty, ^{111}In-DTPA-octreotide was developed. In-111 has a half-life of 2.83 days, emits gamma rays and Auger electrons, which are useful for both imaging and therapy. DTPA binds to the metal ion through four deprotonated carboxylate groups and three tertiary amino groups, and forms an amide bond to the peptide through reaction with an activated carboxylic acid group (Figure 2.3). ^{111}In-DTPA-octreotide was the first peptide receptor agent available on the market, named OctreoScan,® for imaging and therapy.[2, 3]

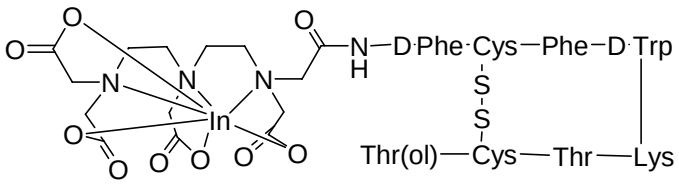

Figure 2.3: ^{111}In-DTPA-octreotide (Octreoscan®)

Since the FDA approval of ^{111}In-DTPA-octreotide (Octreoscan®) for the diagnosis of pancreatic, carcinoid, lung and other cancers, somstostatin receptor expressing tumors have received a lot of attention. Depending on their emissions and properties, researchers used different radiometals, such as ^{90}Y and ^{64}Cu, to produce better imaging and therapy agents.[3-8] To produce kinetically inert radiometal complexes with high physiological stability, they used appropriate chelating agents like DTPA, DOTA, TETA, etc. To improve the biodistribution and receptor binding, the amino acid sequence of octreotide was modified, which led to the evlolution of Tyr^3-octreotate (Figure 2.4).

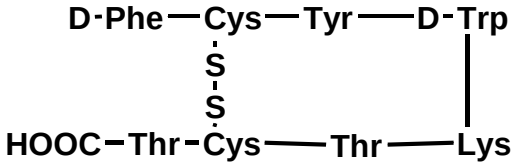

Figure 2.4: Tyr^3-octreotate

Tyr^3-octreotate has a tyrosine instead of a phenylalanine in the third position, and a carboxylic acid instead of an alcohol at the *C*-terminus of octreotide. ^{64}Cu-TETA-Tyr^3-octreotate,[7] described by Anderson et al., showed higher tumor cell uptake compared to ^{64}Cu-TETA-octreotide.[8]

Most of the research to date has used the bifunctional chelate approach, in which a chelating moiety is attached to a receptor-targeting peptide and coordinated to a metal.

The compounds produced by this method showed excellent imaging characteristics but limited therapeutic properties due to poor retention of radioactivity in tumors, requiring the administration of large doses of radioactivity to patients. This resulted in high doses of radiation to the kidneys, the clearance organ, leading to renal toxicity or irreversible renal failure.[9] For example, the use of ^{90}Y-DOTA-Tyr^3-octreotide produced substantial response rates, but with approximately 50% incidence of irreversible renal failure, while the use of ^{111}In-DTPA-octreotide therapy produced negligible toxicity but very low incidence of objective responses.[10] At present, ^{177}Lu-DOTA-Tyr^3-octreotate is emerging as a promising clinic thereapeutic agent by showing considerable efficacy and less evidence of renal toxicity compared to ^{90}Y.[9, 10]

2.2. Goal of These Studies

In the current studies, the aim was to modify somatostatin analogues to improve tumor retention of radioactivity, thereby producing more effective imaging and therapy at lower doses, with minimal amounts of radiation to the kidneys.

2.3. Approach

Targeting improved tumor retention, we investigated the direct metal cyclization approach, where the radiometal is incorporated directly into the peptide sequence. Reported by Giblin et al., Re/Tc were incorporated directly into the disulfide bond of α-MSH peptides.[11,12] The direct metal cyclization approach resulted in a highly stable radiometal-peptide conjugate with higher tumor retention observed than for the bifunctional chelate approach with α-MSH peptides.

This chapter describes the nonradioactive metal labeling of different somatostatin analogues using the direct metal cyclization approach. The purpose of using rhenium is that it is a nonradioactive analogue to both technetium and radioactive rhenium. We incorporated nonradioactive rhenium into the disulfide bond of the cysteine residues in each of the four somatostatin analogues listed below.

(1) Octreotide: $_{D}$Phe-Cys-Phe-$_{D}$Trp-Lys-Thr-Cys-Thr(ol)

(2) Ac-octreotide: Ac-$_{D}$Phe-Cys-Phe-$_{D}$Trp-Lys-Thr-Cys-Thr(ol)

(3) Tyr^{3}-octreotate: $_{D}$Phe-Cys-Tyr-$_{D}$Trp-Lys-Thr-Cys-ThrOH

(4) Ac-Tyr^{3}-octreotate: Ac-$_{D}$Phe-Cys-Tyr-$_{D}$Trp-Lys-Thr-Cys-ThrOH

Where "(ol)" refers to an alcohol *C*-terminus and "OH" refers to an acid *C*-terminus.

2.4. Results and Discussion

This chapter focuses on the incorporation of nonradioactive rhenium into the disulfide bond of the two cysteine residues (Cys-Re-Cys) in each of the four somatostatin analogues. ^{185}Re/^{187}Re is a non radioactive analogue to technetium as well as to the radioactive rhenium (^{186}Re/^{188}Re). Since Re(V) and Tc(V) are highly electron deficient, only good electron donating atoms can form kinetically stable complexes with these centers. Both of these metals form stronger bonds with sulfhydryl groups, amine or amide nitrogens and also with oxygen.[13]

The α-MSH analogues were found to have the metal coordinated to the two Cys sulfhydryls and two nitrogens from nearby amino acid amide or amine groups in the sequence. Based on the information provided by the α-MSH analogues, it was expected that the four somatostatin analogues would also cyclize through bonding of the metal to the thiolato sulfurs and two nitrogen donors from peptide amides or amines.

2.4.1. Synthesis of Rhenium-cyclized Somatostatin Analogues

Syntheses of rhenium-cyclized somatostatin analogues was done by modifying the procedure reported by Giblin et al. [11,12] Rhenium-cyclized somatostatin analogues were obtained by reacting the linear peptides with $[ReOCl_3(OPPh_3)(SMe_2)]$ in an aqueous methanol solution (pH ~8.5) at 65 °C for 60 min.

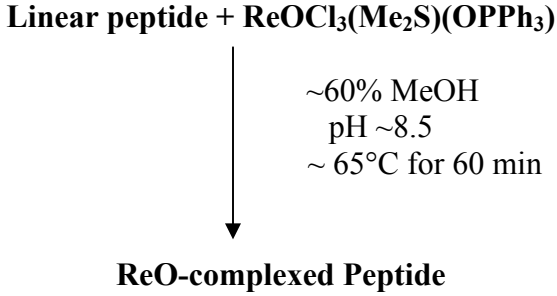

Scheme 2.1: Synthesis of rhenium-cyclized somatostatin analogues

2.4.2. Confirmation of the Formation of Rhenium-cyclized Somatostatin Analogues by LC/MS

The expected mass of the main product for each reaction after synthesis was confirmed by LC-MS. The LC-MS spectrum of each of the four rhenium-cyclized peptides showed three significant peptide peaks (see Figure 2.5 for ReO-octreotide). The major and minor species containing rhenium have the expected mass of the product but dissimilar retention times, yields and mass ionization patterns (Table 2.1). The third peptide product was found to be the Re-free cyclized disulfide compound. The remaining peak was determined to be a decomposition product from the excess Re-starting material.

Re-cyclized peptide	**Gradient**		**Retention time**			**M/Z**	
	(%B)	min	Major	Minor	Re-free disulfide	Major and minor	Disulfide
Octreotide	5-35	45	47.7	33.8	36.1	1221.5	1021.5
Ac-octreotide	26-36	35	12.4	21.8	15.7	1263.1	1061.2
Tyr^3-octreotate	5-35	45	29.2	39.7	30.8	1251.6	1049.5
Ac-Tyr^3-octreotate	20-40	60	15.1	21.5	17.2	1293.7	1091.5

Table 2.1 LC-MS data of Re-cyclized peptides

LC-MS data (Figures 2.5, 2.6, 2.7, 2.8) of the ReO-octreotide showed that the two products found at retention times of 47.7 min and 33.8 min had a m/z of 1221.5 $(M+H)^{1+}$ and of 611.1 $(M+2H)^{2+}$. These values were in good agreement with the calculated values 1221 and 611 for the singly and doubly charged species of the mono-oxo Re complex. This also confirmed that the octreotide formed a complex with the Re oxo core by the loss of four protons. Rhenium has two stable isotopes, ^{185}Re and ^{187}Re. The isotope pattern is qualitatively consistent with the presence of one atom of rhenium per molecule. Also formed in this reaction was a rhenium free disulfide species at a m/z of 1021.5, and an impurity, in the form of triphenyl phosphine oxide dimer (Ph_3PO-$OPPh_3$) at m/z of 557.1.

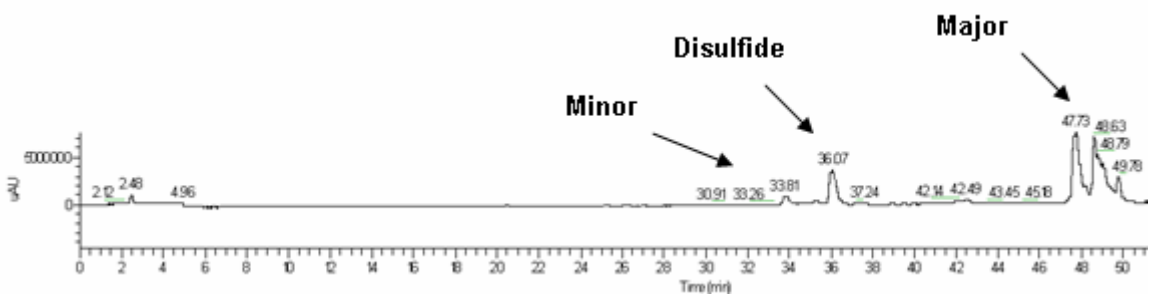

Figure 2.5: LC-MS chromatogram of ReO-octreotide

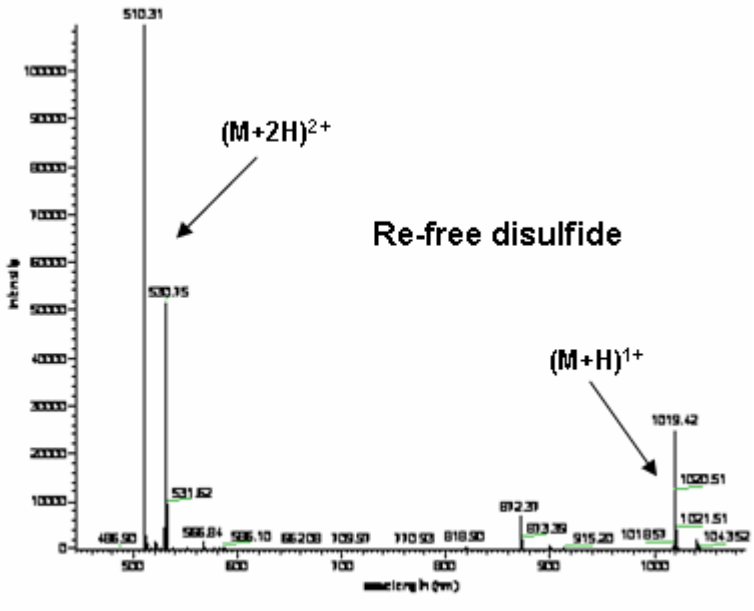

Figure 2.6: LC-MS chromatogram showing Re-free disulfide species of ReO-octreotide

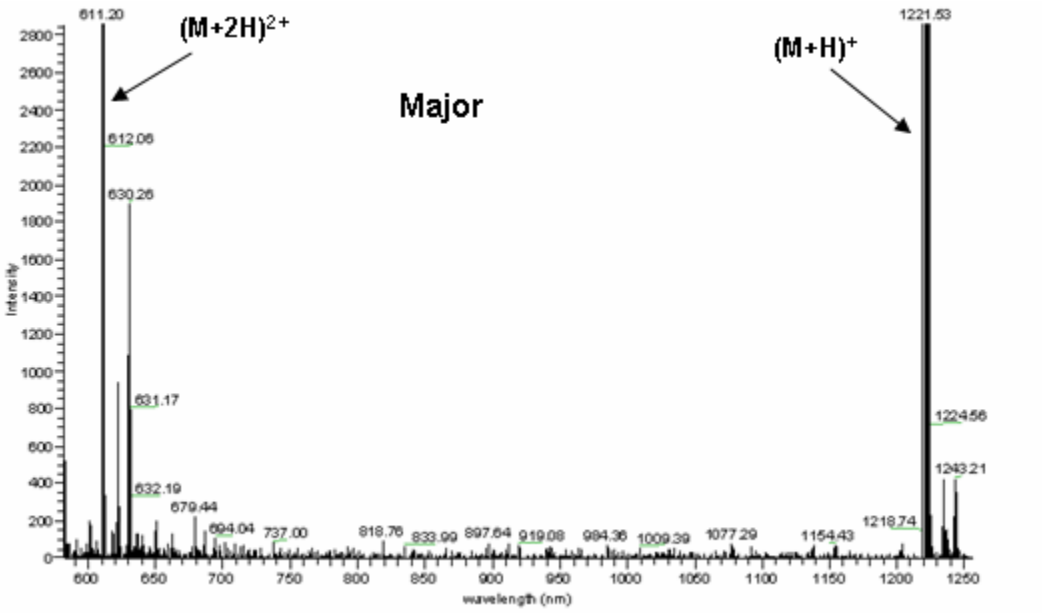

Figure 2.7: LC-MS chromatogram showing major species of ReO-octreotide

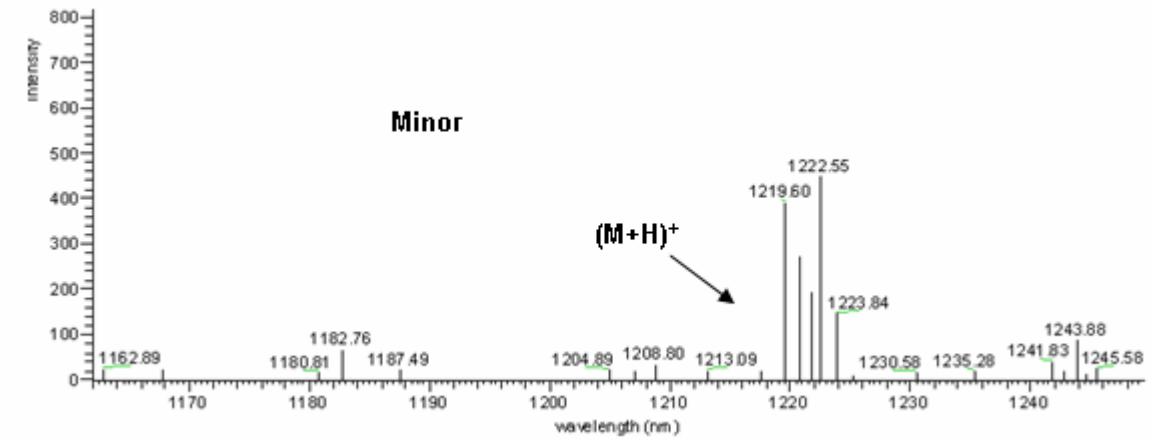

Figure 2.8: LC-MS chromatogram showing minor species of ReO-octreotide

The LC-MS data (Figure 2.9, 2.10, 2.11, 2.12) of the ReO-Tyr^3-octreotate showed that the two products found at retention times of 29.2 min and 39.7 min had a m/z of 1251.6 $(M+H)^{1+}$ and of 626.1 for $(M+2H)^{2+}$. These values were in good agreement with the calculated values of 1251 and 626 for the singly and doubly charged species of the

mono-oxo Re complex. A Rhenium free disulfide product at the retention time of 30.8 min with an m/z of 1049.5 $(M+H)^{1+}$ and an impurity of 49.1 min with m/z of 557.1 were found, consistent with that seen with ReO-octreotide.

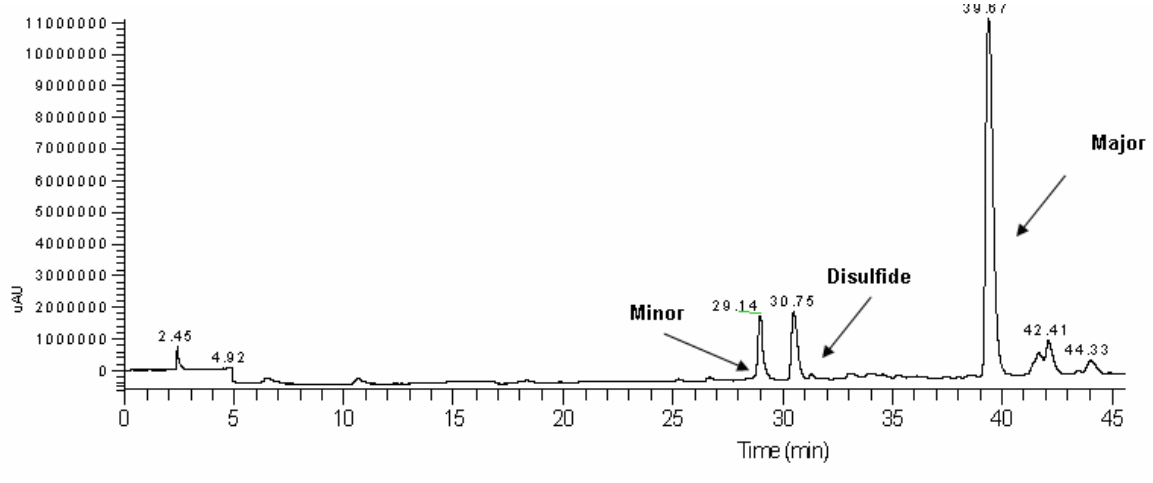

Figure 2.9: LC-MS chromatogram of ReO-Tyr^3-octreotate

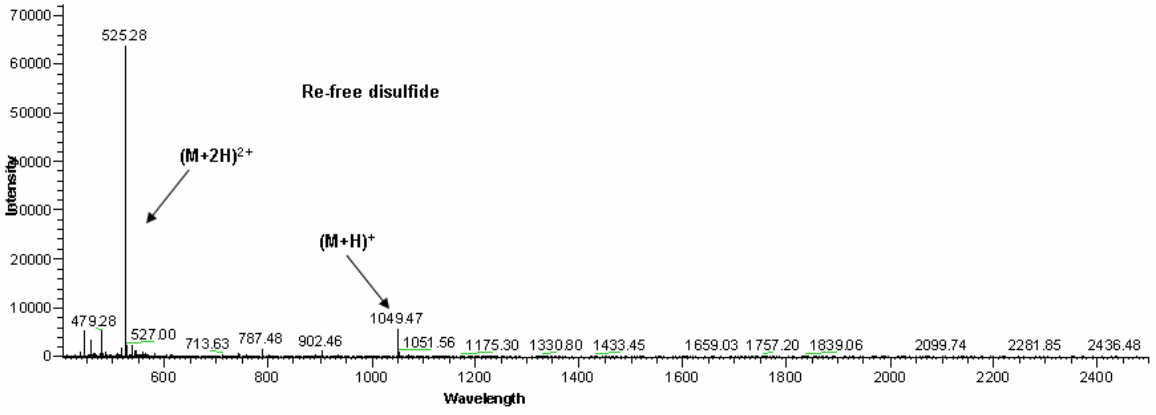

Figure 2.10: LC-MS chromatogram of ReO-Tyr^3-octreotate showing Re-free disulfide

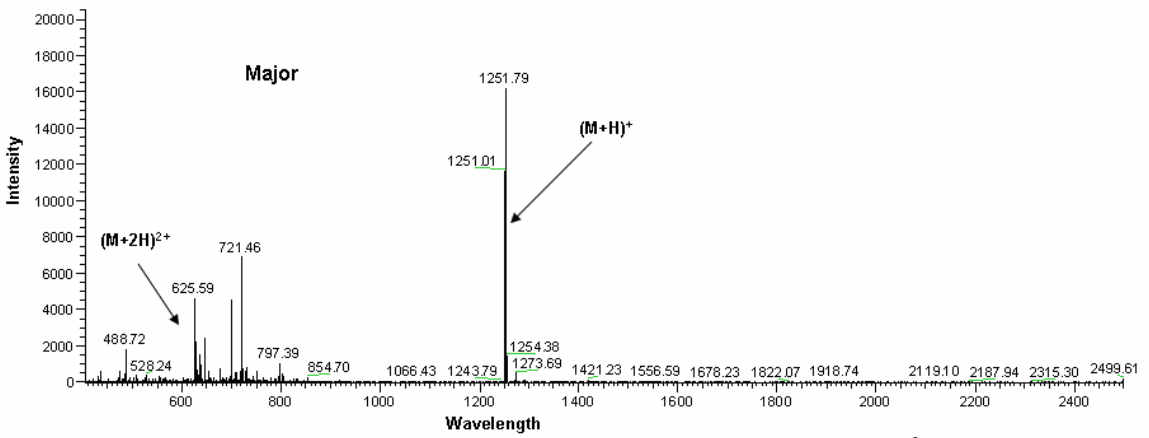

Figure 2.11: LC-MS chromatogram showing major species of ReO-Tyr^3-octreotate

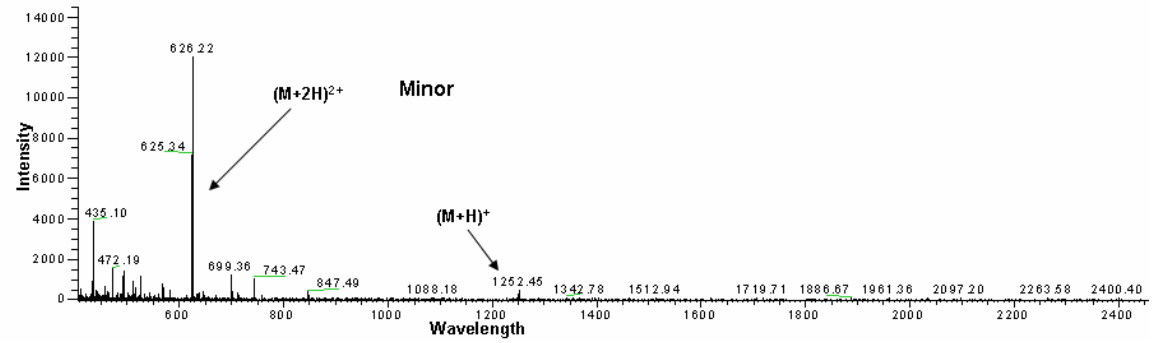

Figure 2.12: LC-MS chromatogram showing minor species of ReO-Tyr^3-octreotate

The LC-MS data (Figures 2.13, 2.14, 2.15, 2.16) of the ReO-Ac-Tyr^3-octreotate showed that there were two species found at retention times of 15.1 min and 21.5 min, which had m/z of 1293.7 $(M+H)^{1+}$ and of 647.4 for $(M+2H)^{2+}$. These values were in good agreement with the calculated value of 1293 and 647 for singly and doubly charged species of the mono-oxo rhenium complex. There was a rhenium free disulfide species at a retention time of 17.2 min with a m/z of 1091.5 $(M+H)^{1+}$, an impurity in the form of triphenyl phosphine oxide (Ph_3PO) was observed at a retention time of 36.2 with a m/z of 278.9 $(M+H)^{1+}$.

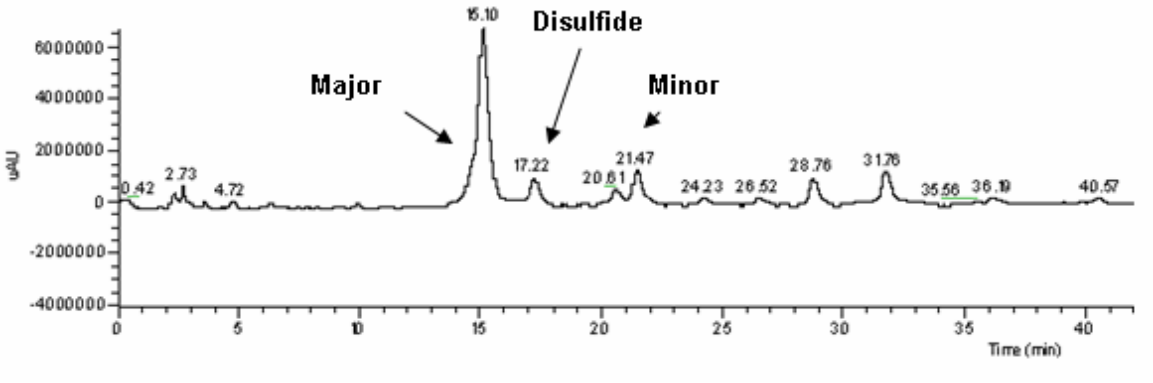

Figure 2.13: LC-MS chromatogram of ReO-Ac-Tyr^3-octreotate

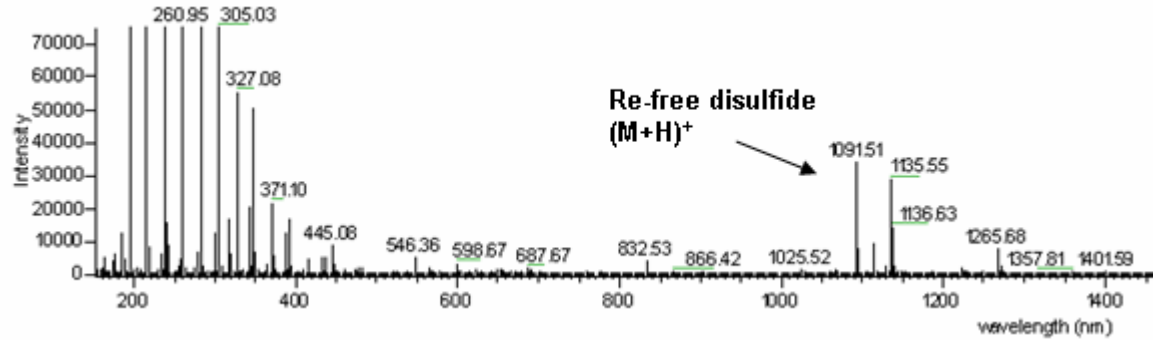

Figure 2.14: LC-MS chromatogram showing Re-free disulfide species of ReO-Ac-Tyr^3-octreotate

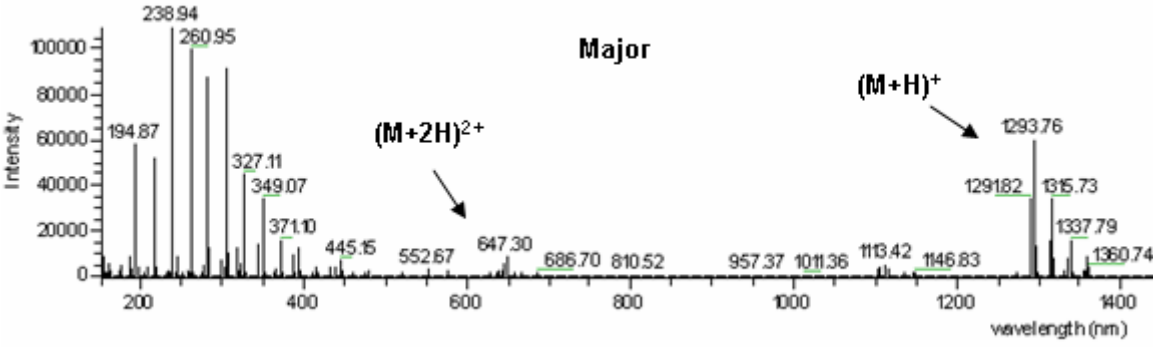

Figure 2.15: LC-MS chromatogram showing major species of ReO-Ac-Tyr^3-octreotate

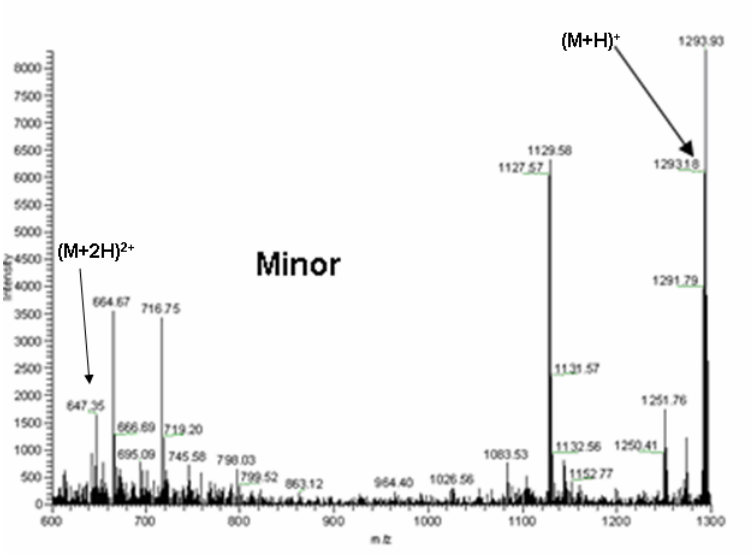

Figure 2.16: LC-MS chromatogram showing minor species of ReO-Ac-Tyr^{3}octreotate

The LC-MS data (Figures 2.17, 2.18, 2.19, 2.20) of ReO-Ac-octreotide showed that there were two species found at retention times of 12.4 min, 21.8 min with m/z values of 1263.3 $(M+H)^{1+}$ and of 632.1 for $(M+2H)^{2+}$. These values were in good agreement with the calculated values of 1263 and 632 for the singly and doubly charged species of the mono-oxo rhenium complex. There was a rhenium free disulfide species at a retention time of 15.7 min and with a m/z of 1061.2 $(M+H)^{1+}$, and an impurity in the form of triphenyl phosphine oxide (Ph_3PO) at a retention time of 24.5 min and with a m/z of 278.9 $(M+H)^{1+}$.

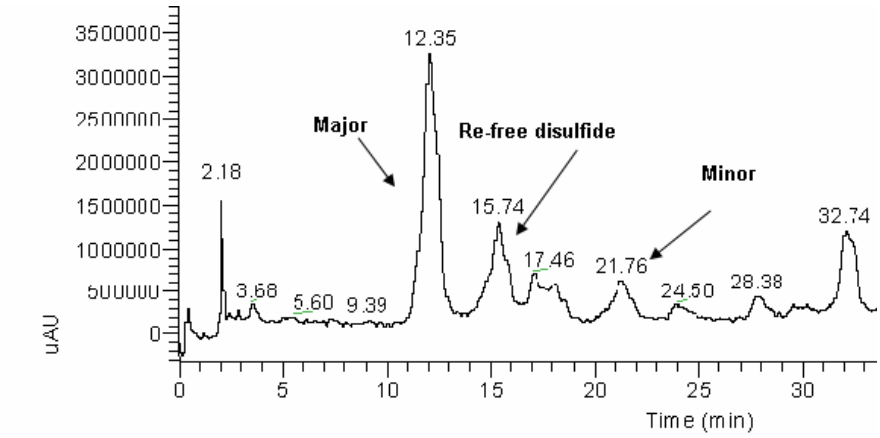

Figure 2.17: LC-MS chromatogram of ReO-Ac-octreotide

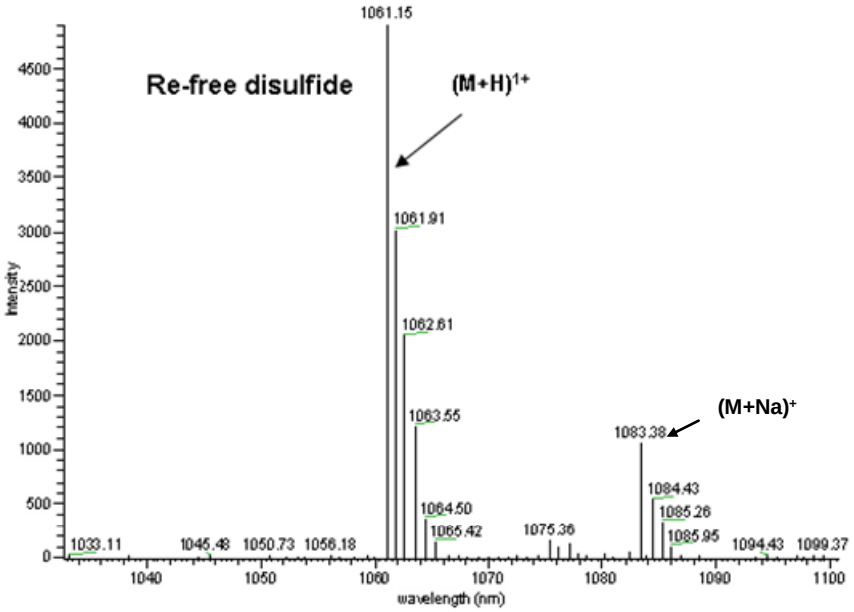

Figure 2.18: LC-MS chromatogram showing Re-free disulfide species of ReO-Ac-octreotide

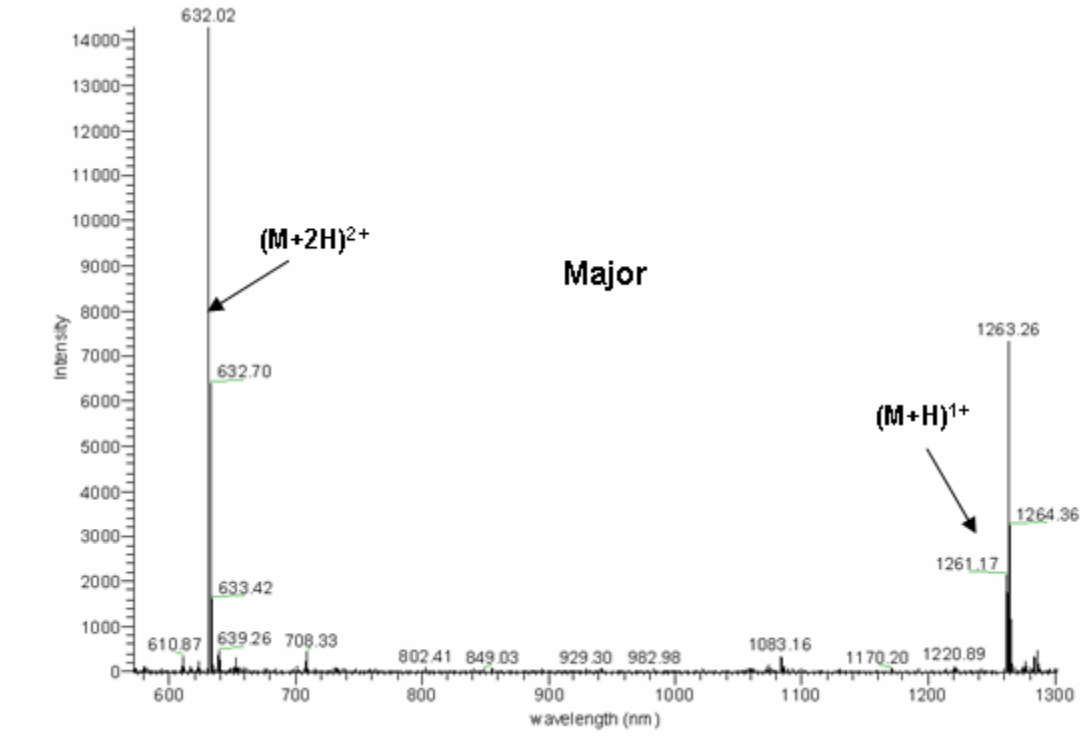

Figure 2.19: LC-MS chromatogram showing major species of ReO-Ac-octreotide

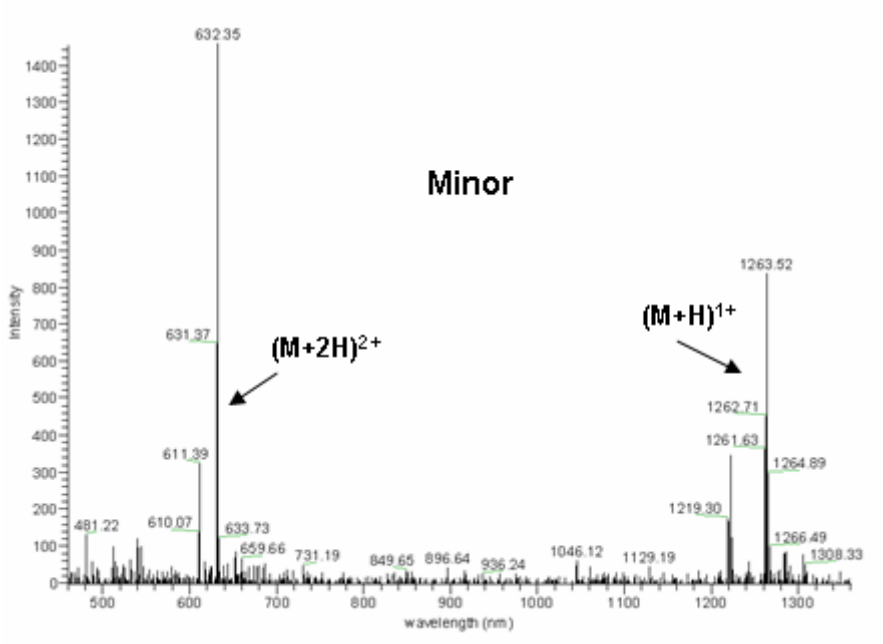

Figure 2.20: LC-MS chromatogram showing minor species of ReO-Ac-octreotide

2.4.3. Purification of Rhenium-cyclized Somatostatin Analogues

Purification of the rhenium-cyclized somatostatin analogues was done by reversed phase C_{18} HPLC. For separation of products in each reaction, different solvent gradients were used (Table 2.2).

Re-cyclized peptide	**Gradient**		**Retention time**		
	(%B)	min	Major	Minor	Re-free disulfide
Octreotide	30-35	35	10.4	3.0	3.5
Ac-octreotide	26-36	35	11.6	15.5	13.0
Tyr^3-octreotate	20-35	35	18.6	6.6	8.1
Ac-Tyr^3-octreotate	22-32	35	12.0	17.0	14.0

Table 2.2: HPLC data of Re-cyclized peptides

B = Acetonitrile/0.1% TFA

There were a few key differences observed in the HPLC retention time studies of ReO-octreotide, ReO-Ac-octreotide, ReO-Tyr^3-octreotate and ReO-Ac-Tyr^3octreotate. The retention time for the minor product was less than the retention time for the major product for both ReO-octreotide and ReO-Tyr^3-octreotate. In the case of ReO-Ac-octreotide, ReO-Ac-Tyr^3-octreotate, the major product retention time was less than the minor product. It was hypothesized that the amine terminus bound to rhenium in the non-acetylated analogues, while it was not involved in the acetylated analogues.

For all four peptides, the rhenium-free disulfide product eluted between the major and minor Re-cyclized products. The retention time for the rhenium-free disulfide was

closer to the minor product for both ReO-octreotide and ReO-Tyr^3-octreotate, while for ReO-Ac-octreotide, and ReO-Ac-Tyr^3-octreotate, the retention time of the rhenium-free disulfide species was closer to the major product.

Based on these HPLC observations, the structures of the major products of ReO-Ac-octreotide and ReO-Ac-Tyr^3-octreotate may be more similar to that of the rhenium-free disulfide species than the major products of ReO-octreotide and ReO-Tyr^3-octreotate.

2.4.4. Retention Time Comparison Studies

We compared retention times for the major products of the four somatostatin analogues on reversed phase HPLC. We used a 35 minute linear gradient of 15-40% solvent B in solvent A with 1 ml/min flow rates for all of the peptides. Our results showed that ReO-Ac-Tyr^3-octreotate elutes at 19.0 minutes, ReO-Tyr^{3}octreotate at 23.9 minutes, and ReO-octreotide at 30 minutes, which agrees with the order of their hydrophilicity (Figure 2.21 and 2.22).

ReO-Ac-Tyr^3-octreotate > ReO-Tyr^3-octreotate > ReO-octreotide

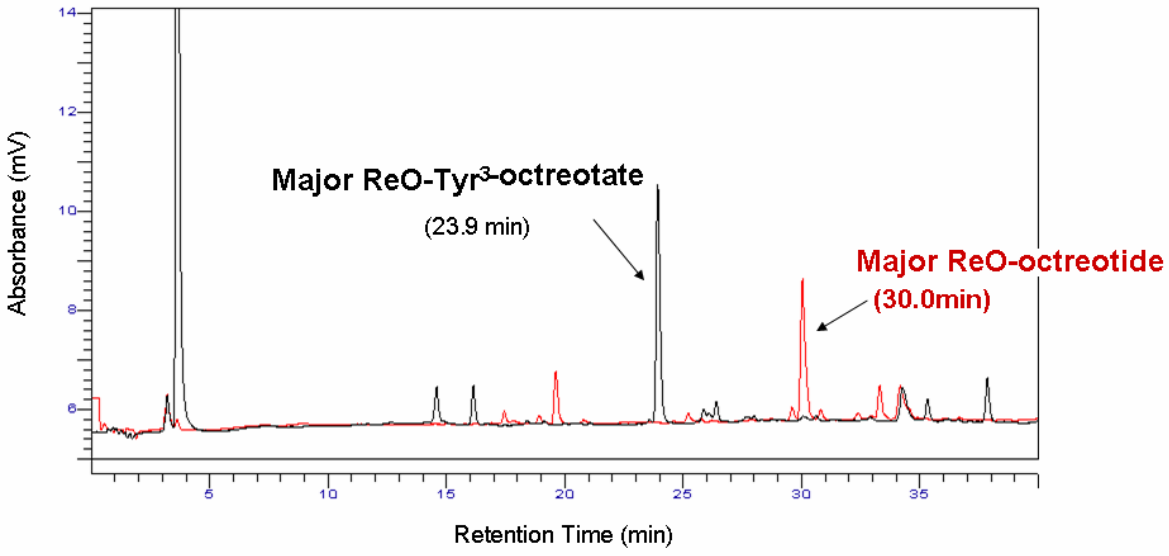

Figure 2.21: Overlay of crude reaction production mixture for ReO-Tyr^3-octreotate and ReO-octreotide

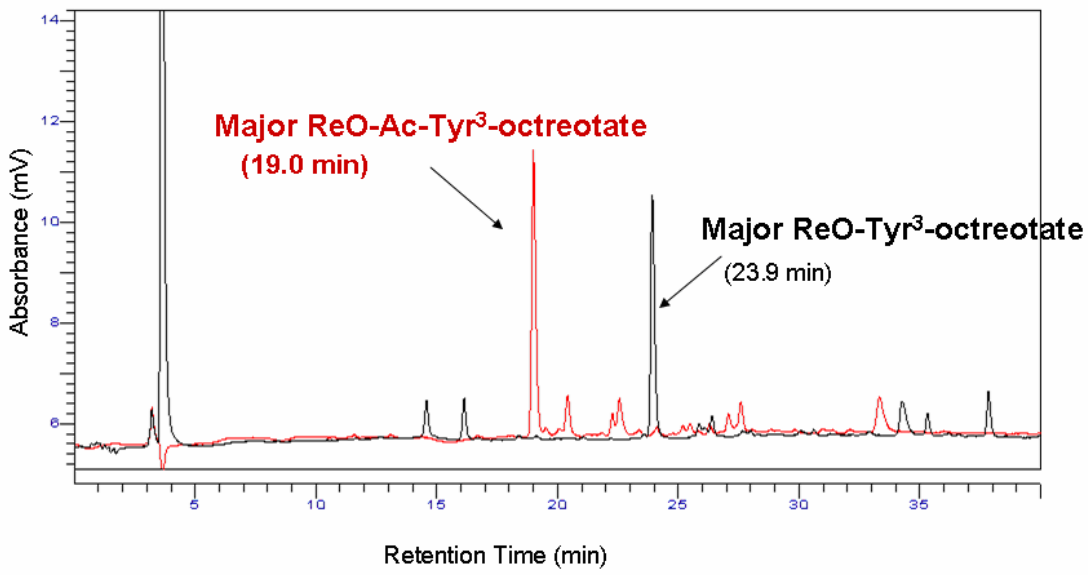

Figure 2.22: Overlay of crude reaction production mixture for ReO-Ac-Tyr^3-octreotate and ReO-Tyr^3-octreotate

Based on the retention times of the main products for each peptide, one can say that the ReO-Ac-Tyr^3-octreotate major product is more hydrophilic than that of ReO-Tyr^3-octreotate, which is more hydrophilic than that of ReO-octreotide. We also observed that the main product of ReO-Ac-Tyr^3-octreotate retention time (19.0) was much closer to the rhenium free disulfide bridged peptide (20.4). This suggests that the acetylation of the *N*-terminus resulted in the formation of a product with more hydrophilicity and possibly a more similar to the disulfide-bridged peptide.

We did not investigate the retention time of the main product of ReO-Ac-octreotide under the same gradient solvent system used for the above three rhenium complexed peptides. But according to the HPLC retention time pattern of ReO-Ac-octreotide under different gradient solvent system it is observed that the elution time profile, mass

ionization patterns of major, minor and rhenium free disulfides peaks are more similar to the ReO-Ac-Tyr^3-octreotate.

Sst Peptide	Retention Time (min)		
	Minor Re product	Disulfide Product	Major Re Product
ReO-octreotide	17.0	19.6	30.0
ReO-Tyr^3-octreotate	14.6	16.1	23.9
ReO-Ac-Tyr^3-octreotate	22.6	20.4	19.0

Table 2.3: Retention time comparison of Re-cyclized peptides

2.4.5. Characterization by ESI-MS

The isolated major products were again verified by Electron Spray Ionization-Mass Spectrometry (ESI-MS).

The ESI-MS of the collected fraction of the major species of ReO-octreotide (Figure 2.23) shows m/z of 1221.6 for $(M+H)^{+1}$, and was in good agreement with the calculated value 1221 for the mono-oxo Re-octreotide.

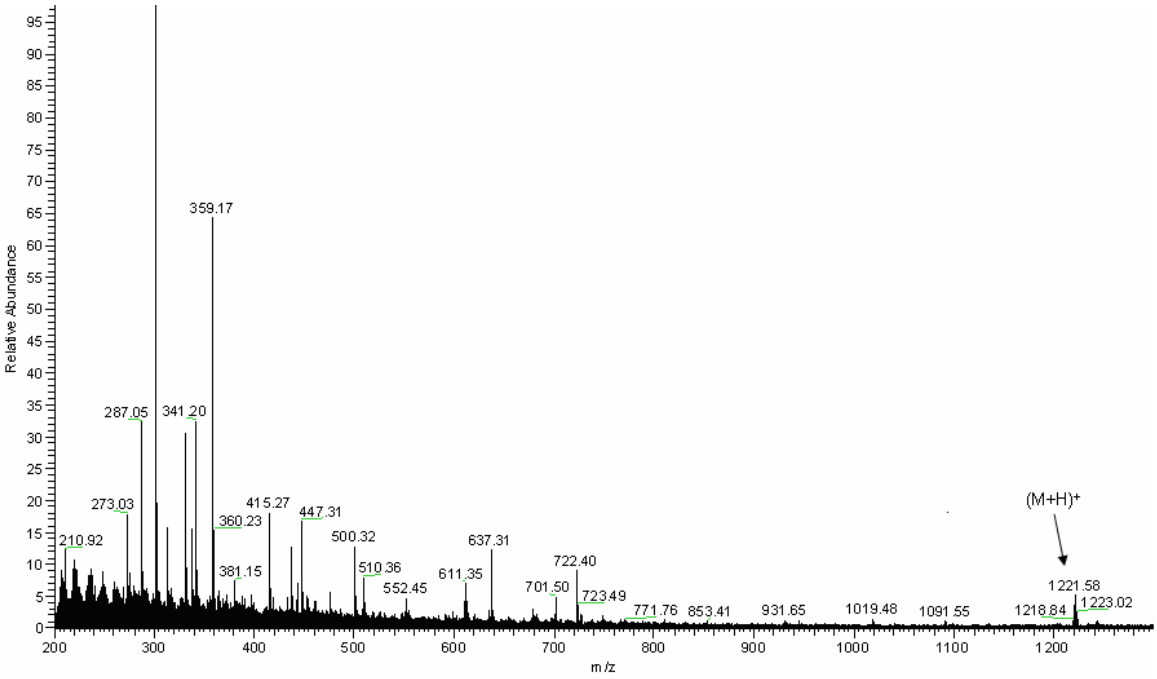

Figure 2.23: ESI-MS spectrum for ReO-octreotide

The ESI-MS of the collected fraction of the major species of ReO-Tyr^3-octreotate (Figure 2.24) shows m/z of 1251.2 for $(M+H)^{+1}$, and was in good agreement with the calculated value 1251 for the mono-oxo Re-Tyr^3-octreotate.

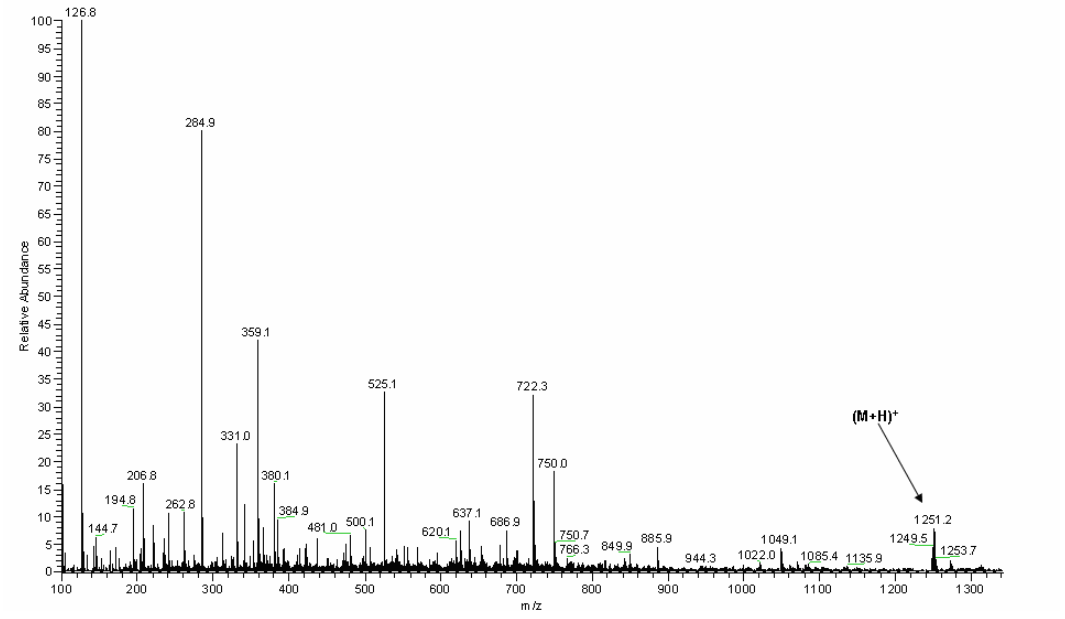

Figure 2.24: ESI-MS spectrum of ReO-Tyr^3-octreotate

The ESI-MS of the collected fraction of the major species of ReO-Ac-Tyr^3-octreotate (Figure 2.25) shows the m/z of 1293.8 for $(M+H)^{+1}$, and was in good agreement with the calculated value 1293 for the mono oxo Re-Ac-Tyr^3-octreotate.

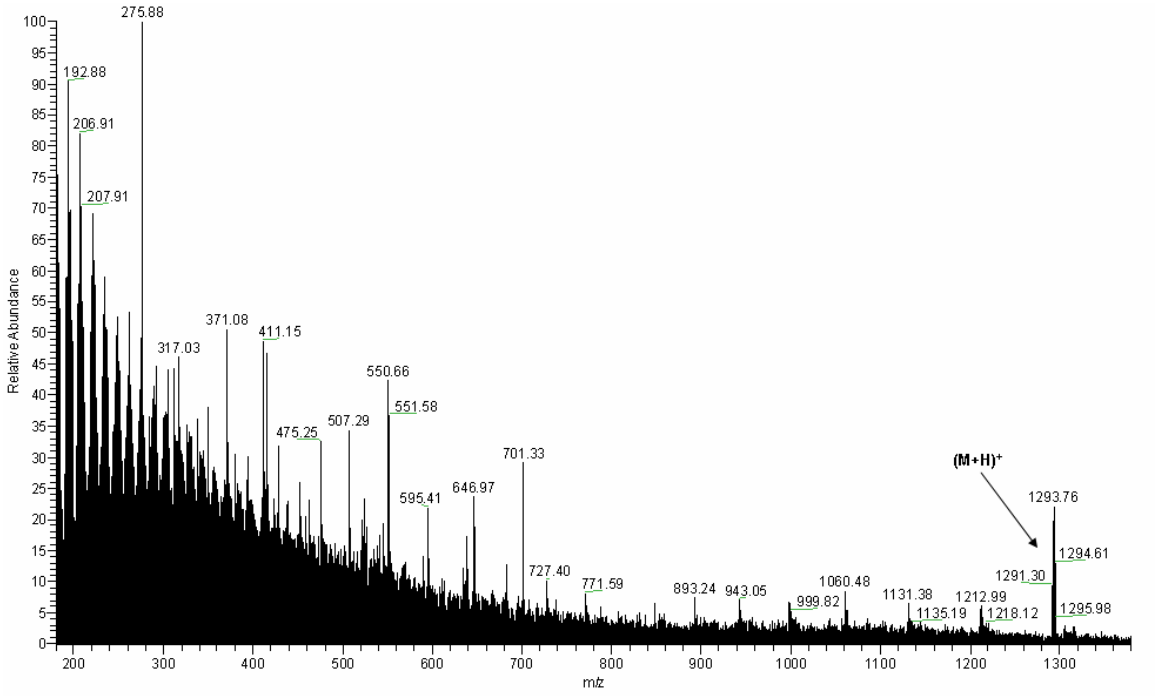

Figure 2.25: ESI-MS spectrum for ReO-Ac-Tyr^3-octreotate

2.5. Conclusions

This chapter describes the synthesis of rhenium labeling of four somatostatin analogues. Confirmation for the formation of the four rhenium-cyclized somatostatin analogues was accomplished with LC-MS. Purification was performed by reversed phase analytical HPLC. The rhenium-cyclized products were further characterized by ESI-MS. Finally, we compared the product retention times of three of the four rhenium-cyclized somatostatin analogue reactions to compare the relative hydrophilicities of the products.

The LC-MS data showed the formation of two cyclic rhenium products with different retention times and mass ionization patterns, which suggest the formation of isomers with different rhenium binding structures. The retention time comparison studies showed that by acetylating the peptide *N*-terminus, a product with increased hydrophilicity, and possibly a structure more similar to the disulfide, was formed as the major product.

^{1}H NMR, ^{1}H-^{13}C HSQC, NOESY, and TOCSY studies done by Dr. Heather Bigott and Dr. Lixin Ma revealed that the N-terminus was involved in binding of peptides with rhenium in cases of both ReO-octreotide and ReO-Tyr^{3}-octreotate and each of these complexes formed two isomers. On the other hand in case of ReO-Ac-octreotide and ReO-Ac-Tyr^{3}-octreotate, the N-terminus was not involved in binding and each of these complexes formed only one isomer.

2.6. Experimental

2.6.1. Synthesis of ReO-octreotide

The ReO-octreotide complex was synthesized using a modified procedure by Giblin, et al.[10,11] The linear octreotide peptide (12.0 mg, 0.0118 mmol) was dissolved in 2 mL of 62% aqueous MeOH solution, and the pH was adjusted to about 8.5 with 0.1 M NaOH. $ReOCl_3(Me_2S)(OPPh_3)$ (11.7 mg, 0.0180 mmol) was added as a solid, and the resultant mint green suspension was refluxed at 65°C for 60 min under N_2 during which it turned to a clear, deep brown/black solution with the formation of a grey/black precipitate. Then the reaction solution was stirred for 4 h at 25°C. The brown colored solution was transferred to a test tube. This brown colored solution, on centrifugation, gave a brownish-black precipitate at the bottom of the test tube, leaving a brown solution on top.

This brown solution, on passing through a 0.22 μm filter (HT Tuffryn membrane), gave a clear brown solution. This solution was dried under gentle N_2 flow yielding a brown residue with orange tones.

2.6.2. LC-MS confirmation of ReO-octreotide

We prepared a 1 mg/mL solution of the crude product with 1:1 solvent A: solvent B (H_2O/0.1%TFA: AcN/0.1%TFA). The LC-MS chromatograms were obtained using a linear gradient and a flow rate of 1 ml/min, in which the concentration of solvent B in solvent A was altered. The gradient used for the separation was as follows: 5-35% B in 45 minutes, 35-95% B in 5 minutes, held for 10 minutes at 95% B then back to initial conditions (5% B) in 2 min, and held for 10 min at 5% B. Channel A was set at 214 nm and channel B at 280 nm for UV detection.

2.6.3. Purification of ReO-octreotide

A Vydak protein and peptide C_{18} column with a length of 25 cm and a diameter of 46 mm was used for the purification. The injection loop capacity was 10 μL, the flow rate was set at 1 mL/min, and the elution profile was monitored at 280 nm. The gradient used for this separation was as follows: 30-35% B in 35 minutes, 35-95% B in 5 minutes, held for 10 min at 95% B, then back to initial conditions (30% B) in 5 min. The retention time for the major species of ReO-octreotide under this gradient was 10.4 minutes (Figures 2.26, 2.27).

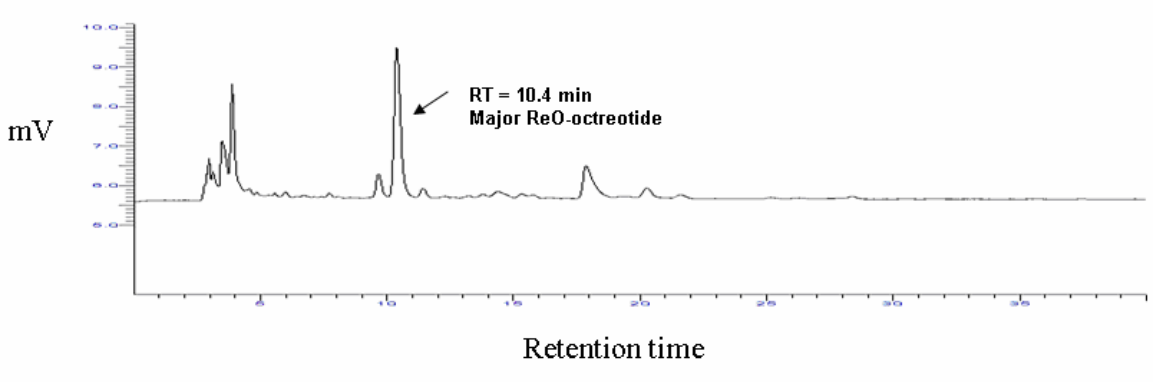

Figure 2.26: HPLC chromatogram of ReO-octreotide before purification

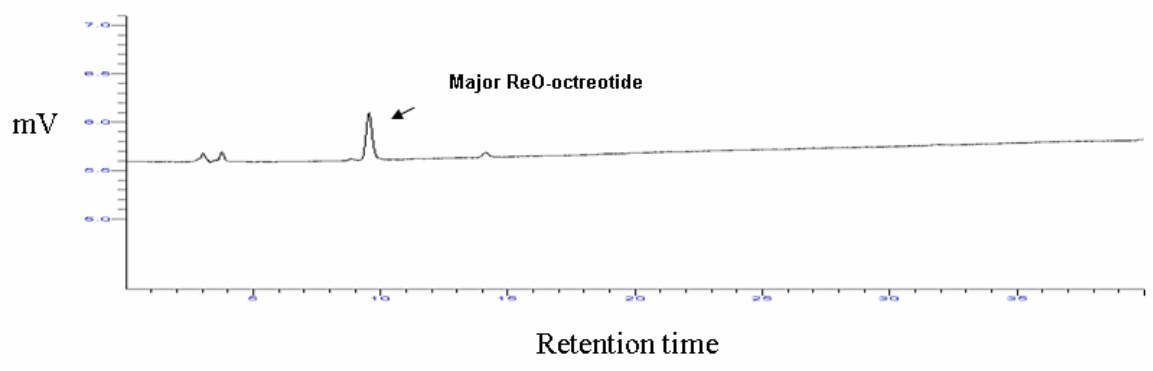

Figure 2.27: HPLC chromatogram of ReO-octreotide after purification

Four fractions of major ReO-octreotide species were collected and centrivapped to remove solvents. The dried fraction 3 was used for further analysis and characterization. Fraction 3 was dissolved in 20 µL of solvent A and 20 µL of solvent B and half of the volume was characterized by ESI-MS and the remaining 20 µL was injected into the HPLC. The retention time for the collected species and formation of a single peak on HPLC showed that collected fraction 3 does not contain any other species. The collected single peak for fraction 3 was submitted to mass spectrometry for further confirmation.

2.6.4 Synthesis of ReO-Tyr^3-octreotate

ReO-Tyr^3-octreotate was synthesized in a similar manner to ReO-octreotide with some minor changes. In this synthesis, linear peptide (9 mg, 0.00856 mmol) was dissolved in 2 mL of 75% aqueous MeOH solution. $ReOCl_3(Me_2S)(OPPh_3)$ (9 mg, 0.01386 mmol) was added to the peptide solution as a solid and gave a mint green suspension. This suspension, on refluxing at 65°C under N_2, became a clear dark brown solution which turned to dark brown within 14 min. This reaction was refluxed for 60 more minutes for completion. Then the reaction solution was stirred for 4 h at 25 °C. The brown colored solution was transferred to test tube. This brown colored solution, on centrifugation, gave a brownish-black precipitate at the bottom of the test tube, leaving a brown solution on top. This brown solution, on passing through a 0.22 μm filter (HT Tuffryn membrane), gave a clear brown solution, which was dried under gentle N_2 flow, and resulted in a brown residue with orange tones.

2.6.5. LC-MS confirmation of ReO-Tyr^3-octreotate

We prepared a 1 mg/mL solution of the crude product with 1:1 solvent A: solvent B (H_2O/0.1%TFA: AcN/0.1%TFA). The solvent system, flow rate, gradient used for the separation, injection volume and channel setting were same as for ReO-octreotide.

2.6.6. Purification of ReO–Tyr^3-octreotate

The properties and behavior of the column, dimensions, injection loop capacity, solvent system, flow rate, etc., were the same as described for the purification of ReO-octreotide. The gradient used for this separation was as follows: 20-35% B in 35 minutes, 35-95% B in 5 minutes, held for 10 min at 95% B, and then back to initial

conditions (20% B) in 5 min. The retention time for the major species of ReO-Tyr^3-octreotate under this gradient was 18.60 min (Figures 2.28, 2.29).

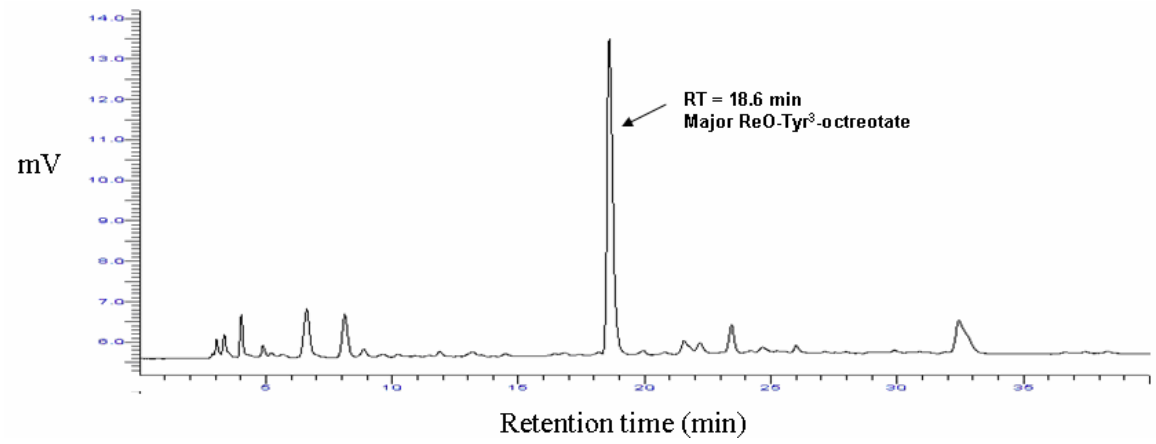

Figure 2.28: HPLC chromatogram of ReO-Tyr^3-octreotate before purification

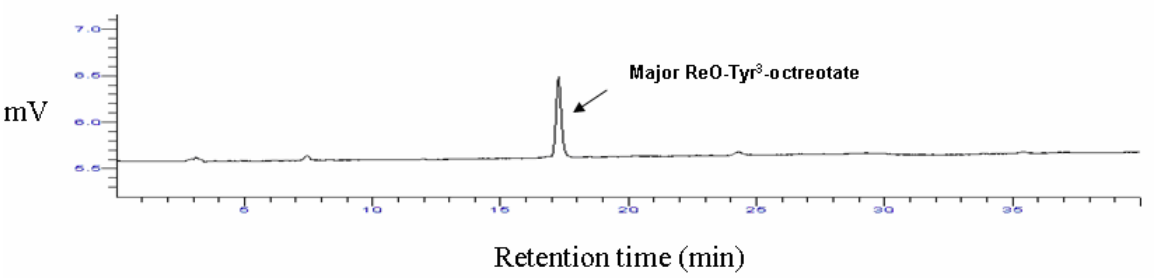

Figure 2.29: HPLC chromatogram of ReO-Tyr^3-octreotate after purification

Three fractions of the major ReO-Tyr^3-octreotate peak were collected and centrivapped to remove the solvents. Fraction 1 was dissolved in 20 µL of solvent A and 20 µL of solvent B and vortexed. Half of the volume was characterized by ESI-MS, and the remaining 20 µL was injected into the HPLC and run with the same gradient used to isolate this species. The retention time and single peak observed by HPLC showed that the collected fraction 1 was pure.

2.6.7. Synthesis of ReO-Ac-Tyr^3-octreotate

ReO-Ac-Tyr^{3}octreotate was synthesized in a similar manner to ReO-octreotide and ReO-Tyr^3-octreotate. In this synthesis linear peptide (9.5 mg, 0.0087 mmol) was dissolved in 2 mL of 75 % aqueous MeOH solution. $ReOCl_3(Me_2S)(OPPh_3)$ (8.7 mg, 0.013 mmol) was added to the peptide solution as a solid and gave a mint green suspension. This suspension on refluxing at 65 °C under N_2, became a cloudy solution with orange tan which turned to orange-brown with in 3 min. This reaction was allowed to run for 60 more minutes for completion. Then reaction solution was stirred for 4 h at 25 °C. The brown solution was transferred to a test tube, and on centrifugation gave a brownish black precipitate at the bottom of the test tube leaving a brown solution on top. This brown solution, on passing through a 0.22 μm filter (HT Tuffryn membrane), gave clear brown solution, which was dried under gentle N_2 flow to give a brown residue with orange tones.

2.6.8. LC-MS Confirmation of ReO-Ac-Tyr^3-octreotate

A 1 mg/mL solution of the processed compound was prepared and dissolved in 1:1 solvent A: solvent B (H_2O/0.1%TFA: ACN/0.1%TFA). The solvent system, flow rate and injection volume was same as used for separating both nonradioactive ReO-octreotide and ReO-Tyr^3-octreotate.

2.6.9. Purification of ReO-Ac-Tyr^3-octreotate

The gradient used for the separation was as follows: 22-32% B in 35 minutes, 32-95% B in 5 minutes, held for 15 min at 95% B and then back to initial conditions (22%

B) in 5 min. The retention time for the major species of ReO-Ac-Tyr^{3}octreotate under this gradient was 12.0 min (Figures 2.30, 2.31).

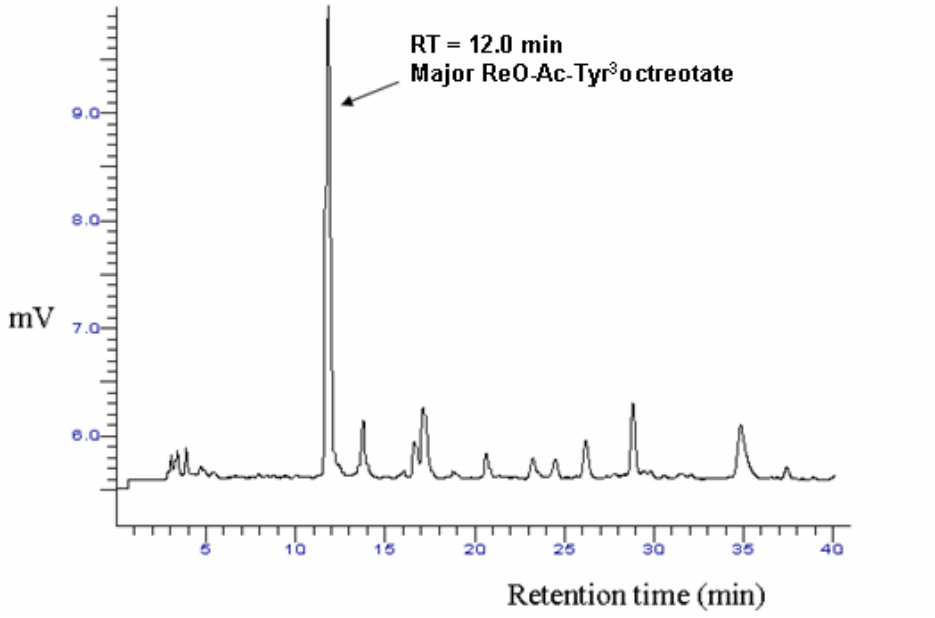

Figure 2.30: HPLC chromatogram of ReO-Ac-Tyr^3-octreotate before purification

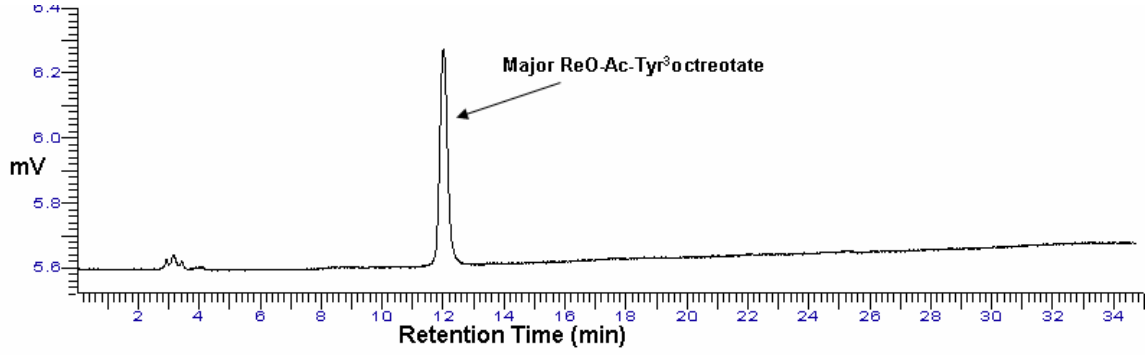

Figure 2.31: HPLC chromatogram of ReO-Ac-Tyr^{3}octreotate after purification

Three fractions of the major ReO-Ac-Tyr^{3}octreotate peak were collected and centrivapped to remove the solvents. Fraction 2 was dissolved in 20 µL of solvent A and 20 µL of solvent B and vortexed. Half of the volume was characterized by ESI-MS, and

the remaining 20 μL was injected into the HPLC and run with the same gradient used to isolate this species. The retention time and a single peak observed on the HPLC showed that the collected fraction 2 was pure.

2.6.10. Synthesis of ReO-Ac-octreotide

ReO-Ac-Tyr^{3}octreotate was synthesized in a similar manner to ReO-octreotide, ReO-Tyr^3-octreotate and ReO-Ac-octreotide. In this synthesis, linear peptide (10.0 mg, 0.009407 mmol) was dissolved in 2 mL of 62 % aqueous MeOH solution and then 500 μL of 70 % aqueous MeOH , and the pH was adjusted to about 8.7 with 0.1 M NaOH. $ReOCl_3(Me_2S)(OPPh_3)$ (9.4mg, 0.01448 mmol) was added to the peptide solution as a solid and gave a mint green suspension. This suspension, on refluxing at 65 °C under N_2, became a cloudy orange tan solution, which turned to orange-brown within 3 min. This reaction was allowed run for 60 more minutes for completion, and then reaction solution was stirred for 4 h at 25 °C. The brown solution was transferred to test tube, and on centrifugation gave a brownish black precipitate at the bottom of the test tube leaving a brown solution on top. This brown solution, on passing through a 0.22 μm filter (HT Tuffryn membrane), gave a clear brown solution, which was dried under gentle N_2 flow to yield a brown residue with orange tones.

2.6.11. LC-MS Confirmation of ReO-Ac-octreotide

A 1 mg/mL solution of the processed compound was prepared and dissolved in 1:1 solvent A: solvent B (H_2O/0.1%TFA: ACN/0.1%TFA). The solvent system, flow rate, injection volume was same as used for separating nonradioactive ReO-octreotide, ReO-Tyr^3-octreotate and ReO-Ac-Tyr^3-octreotate.

2.6.12. Purification of ReO-Ac-octreotide

The gradient used for the separation was 26-36% B in 35 minutes. The retention time for the major species of ReO-Ac-octreotide under this gradient was 11.7 min (Figures 2.32, 2.33)

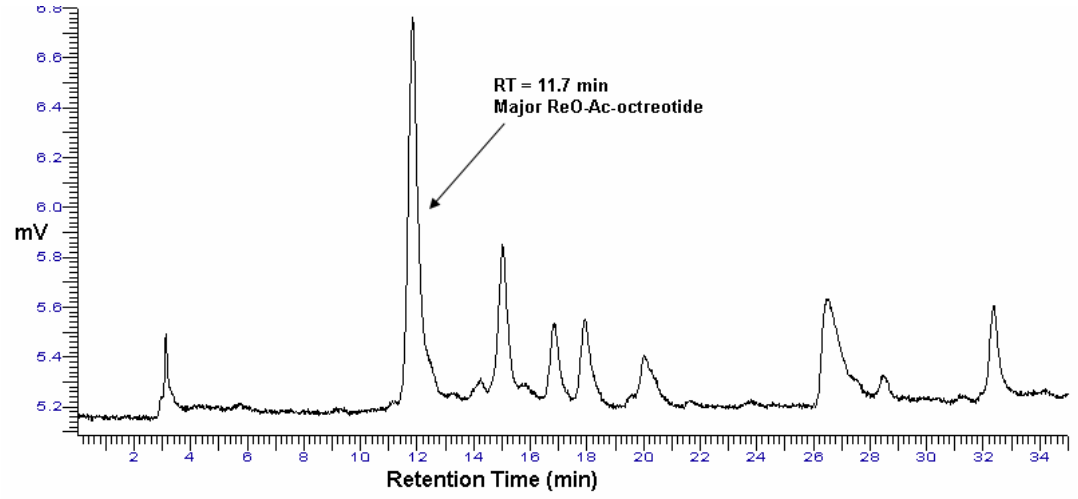

Figure 2.32: HPLC chromatogram of ReO-Ac-octreotide before purification

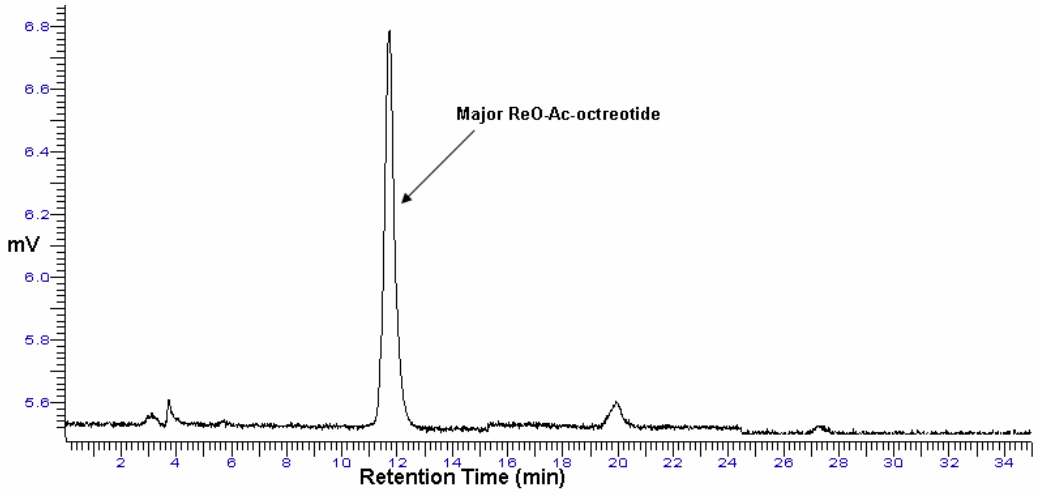

Figure 2.33: HPLC chromatogram of ReO-Ac-octreotide after purification

Three fractions of the major ReO-Ac-octreotide peak were collected and centrivapped to remove the solvents. Fraction 2 was dissolved in 20 µL of solvent A and 20 µL of solvent B and vortexed. Half of the volume was characterized by ESI-MS, and the remaining 20 µL was injected into the HPLC and ran with the same gradient used to isolate this species. The retention time and a single peak observed on the HPLC showed that the collected fraction 2 was pure.

References

1) Gisbert Weckbecker.; Ian Lewis.; Rainer Albert.; Herbert A.; Schmid.; Daniel Hoyer and Christian Bruns. Opportunities in somatostatin research: Biological, Chemical and Therapeutic Aspects. *Nature Rev*. **2003**, 2, 999-1017.

2) Bakker, W. H.; Albert, R.; Bruns, C.; Breeman, W. A. P.; Hofland, L. J.; Marbach, P.; Pless, J.; Pralet, D.; Stoltz., B.; Koper, J. W.; Lamberts, S. W. J.; Visser, T. J. and Krenning, E.P. [Indium-111-DTPA-D-Phe-1]-octreotide, a potential radiopharmaceutical for imaging somatostatin receptor positive tumors: Synthesis, radiolabeling, and in *vitro* validation. *Life Sci*. **1991,** 49, 1583-1591.

3) de Jong, M.; Breeman, W. A. P.; Bakker, W. H.; Kooij, P. P. M.; Bernard, B. F.; Hofland, L. J.; Visser, T. J.; Srinivasan, A.; Schmidt, M. A.; Erion, J. L.; Bugaj, J. E; Macke, H. R. and Krenning, E. P. Comparison of ^{111}In-labeled somatostatin analogs for tumor scintigraphy and radionuclide therapy. *Cancer Res*. **1998,** 58, 437-441.

4) de Jong, M.; Bakker, W. H.; Krenning, E. P.; Breeman, W. A. P.; Van Der Pluijm, M. E.; Bernard, B. F.; Visser, T. J.; Jermann, E.; Behe, M.; Powell, P. and Macke, H. R. Yttrium-90 and indium-111 labeling, receptor binding and biodistribution of [DOTA0, D-Phe1, Tyr3]octreotide, a promising somatostatin analog for radionuclide therapy. *Eur. J. Nucl. Med.* **1997**, 24, 368-371.

5) Heppler, A.; Froidevaux, S.; Macke, H. R.; Jermann, E.; Behe, M.; Powell, P. and Henning, M. Radiometal-labelled macrocyclic chelator-derivatized somatostatin analogue with superb tumor-targeting properties and potential for receptor-mediated internal radiotherapy. *Chem. Eur. J.* **1999**, 5, 1974-1981.

6) Lewis, J. S.; Lewis, M. R.; Srinivasan, A.; Schmidt, M. A.; Wang, J. and Anderson, C. J. Comparison of four ^{64}Cu-labeled somatostatin analogs *in vitro* and in a tumor bearing rat model: evaluation of new derivatives of positron emission tomography imaging and targeted radiotherapy. *J. Med. Chem.* **1999,** 42, 1341-1347.

7) Lewis, J. S.; Lewis, M. R.; Srinivasan, A.; Schmidt, M. A.; Schwarz, S. W.; Morris, M. M.; Miller, J. P. and Anderson , C. J. Radiotherapy and dosimetry of ^{64}Cu-TETA-Tyr^3-octreotate in a somatostatin receptor-positive, tumor-bearing rat model. *Clin Cancer Res.* **1999,** 5, 3608-3616.

8) Anderson, C. J.; Dehdashti, F.; Cutler, P. D.; Schwarz, S. W.; Laforest, R.; Bass, L. A.; Lewis, J. S. and McCarthy, D. W. ^{64}Cu-TETA-octreotide as a PET imaging agent for patients with neuro endocrine tumors. *J. Nucl.Med.* **2001,** 42, 213-221.

9) Lewis, J. S.; Wang M.; Laforest, R.; Wang, F.; Erion, J.L.; Bugaj, J.e.; Srinivasan, A. and Anderson, C. J. Toxicity and Dosimetry of ^{177}Lu-DOTA-Y3-octreotate in a rat model. *Int. J. Cancer.* **2001,** 94, 873-877.

10) Kwekkeboom, D. J.; Bakker, W. H.; Kooji, P. P. M.; Konijnenberg, M. W.; Srinivasan, A.; Erion, J. L., Schmidt, M. A.; Bugaj, J. L.; de Jong, M. and Krenning, E. P. *Eur. J. Nucl. Med.* **2001**, 28, 1319-1325.

11) Giblin, M. F.; Wang, N.; Jurisson, S. S. and Quinn, T. P. Synthesis and Characterization of rhenium complexed α-melanotropin analogs. *Bioconjugate Chem.* **1997**, *8*, 347-353.

12) Giblin, M. F.; Wang, N.; Hoffman, T. J.; Jurisson, S. S. and Quinn, T. P. Design and characterization of α-melanotropin peptide analogs cyclized through rhenium and technetium metal coordination. *Proc. Natl. Acad. Sci. U.S.A.* **1998,** 95, 12814-12818.

13) Vanbilloen, H. P.; Bormans, G. M.; De Roo, M. J. and Verbruggen, A. M. Complexes of technetium-99m with tetrapeptides, a new class of ^{99m}Tc-labelled agents *Nucl. Med. Biol.* **1995**, 22, 325-338.

CHAPTER 3

Rhenium Amine Complexes

3.1 Introduction

The coordination chemistry of technetium and rhenium is similar since they belong to the second and third transition series of Group 7, respectively.[1] However, there are some differences in their chemical properties, which lead to biological distinctions between analogous complexes.

Because of the similarity in the coordination chemistry of rhenium and technetium, the knowledge of the biodistribution of technetium complexes helps in understanding of the rhenium complexes, behavior and *vice versa.* Rhenium is readily available in non-radioactive form, so the basic research on rhenium can be done in non-radioactive environments, which can then eventually be extended to technetium.[2]

Complexes containing oxygen and nitrogen multiple bonds dominate the chemistry of the +5 oxidation state of rhenium. This is because O^{2-} and N^{3-} donate π electrons, thereby stabilizing the high oxidation state of the metal by neutralizing the high formal charge on the metal center.[3,4] Re(V) forms a large number of stable diamagnetic complexes in which the metal forms multiple bonds to oxygen or nitrogen. For instance, one effective way of stabilizing the Re(V) centre in aqueous solution is as the dioxo ($[O=Re=O]^{+}$) core.[5] In some cases, one oxo group and four anionic ligands can satisfy the high-charge requirements of Tc(V) and Re(V) centers, and some of these complexes may weakly bind a ligand *trans* to the oxo.[6]

Many Re/Tc(V) complexes are used as radiopharmaceuticals. For example, [^{99m}TcO(*d,l*-HMPAO)] (Figure 3.1), a Tc(V) complex containing Tc-N bonds, is used as a radiopharmaceutical for cerebral perfusion imaging.[7] This is a neutral lipophilic complex, and has the ability to cross the blood brain barrier (BBB). After diffusing into the brain, it transforms into a more hydrophilic species that cannot diffuse out of the brain, and thus is retained in the brain. Only the *d,l*-isomers are transformed to a more hydrophilic species at a sufficient rate so they cannot diffuse out of the brain. The *meso*-isomer undergoes this transformation at a much slower rate and diffuses out of the brain.

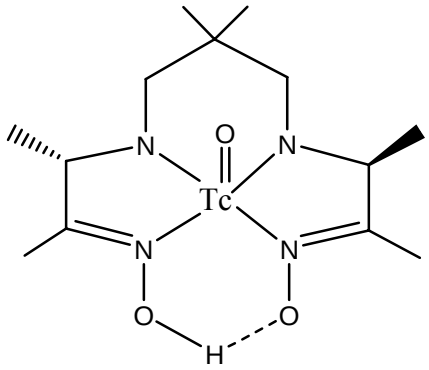

Figure 3.1: ^{99m}TcO(*d,l*-HMPAO)

The exact mechanism of action of this radiopharmaceutical is not known. The ligand of the complex may be displaced and new bonds may be formed between the metal and tissue in the brain, or there may be some interactions that trap the complex in the brain.[7]

Another brain imaging agent currently being used is ^{99m}Tc(*l,l*-ECD) (Figure 3.2). Tc(V) is complexed with a tetradentate diamino-ethane-dithiolato ligand. This complex is also neutral and crosses the blood brain barrier, where it is trapped inside the brain. The mechanism involved in trapping this radiopharmaceutical is known. Esterase enzymes hydrolyze ester groups on the complex resulting in a more hydrophilic and

charged complex, which cannot diffuse out of the brain. Only the *l,l* isomer undergoes enzyme hydrolysis. The *d,d* isomer does not undergo enzyme hydrolysis and diffuses back across the blood brain barrier.[8.]

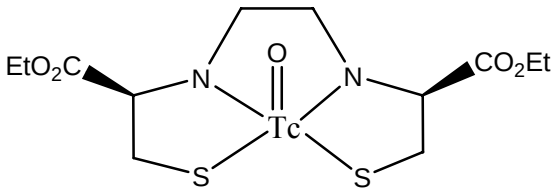

Figure 3.2: ^{99m}TcO(*l,l*-ECD)

3.2 Aim of the Study

This chapter focuses on the syntheses of two Re(V) diamine complexes, their characterization and determination of the acid dissociation constants (pKa). Engelbrecht[9] observed that with increased functionalization of the ethylenediamine type ligands coordinated to a Re(V) metal center, there was a decrease in the pKa values of the oxo group.

Aimed at confirming the observation that the functionalization of ethylenediamine type ligands coordinated to a Re(V) metal center results in decreases in the pKa values of the oxo group, we synthesized two rhenium(V) complexes containing amine ligands and investigated the steric and electronic impact of these ligands on the Re(V) dioxo center. One complex was with 1,2-diamino-2-methylpropane and the other was with N,N-dimethyl ethylenediamine (Figure 3.3).

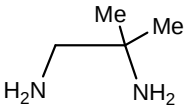

1,2-Diamino-2-methyl Propane

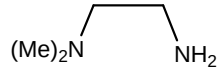

N,N-Dimethylethylenediamine

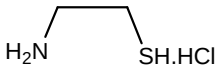

2-Aminoethanethiolate

Figure 3.3: Ligands used for preparing Re-complexes

This chapter also investigates on synthesis of a Re(V) complex with an aminothiol ligand. This Re(V) complex is further reduced to Re(III) with triethylphosphine. Re(III) is kinetically more inert than Re(V). As Re(III) is kinetically inert, it is expected to be more stable *in vivo* and therefore it may have a greater value in therapeutic radiopharmaceuticals.

3.3 Results and Discussion

3.3.1 Synthesis of $[ReO(OH)(H_2NCH_2C(CH_3)_2NH_2)_2](ClO_4)_2$ (2)

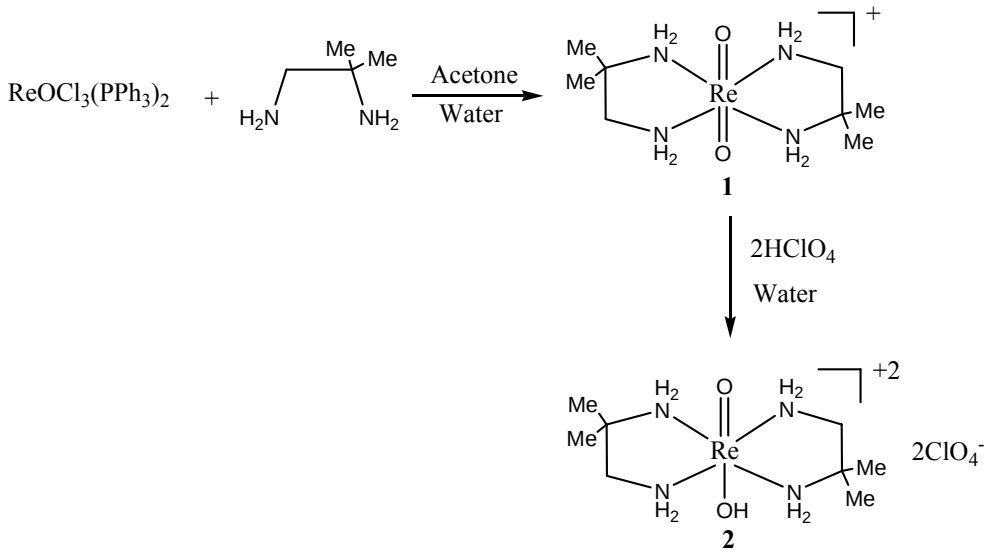

Scheme 3.1: Synthetic route for $[ReO(OH)(H_2NCH_2C(CH_3)_2NH_2)_2](ClO_4)_2$ (2)

Complex **2** was synthesized by modifying the synthetic route reported by Engelbrecht.[9] (Scheme 3.1). Excess 1,2–diamino-2-methylpropane (40 fold) was used to obtain complex **1**. Complex **1** was characterized by ^{1}H-NMR and IR spectroscopies. The IR stretch at 821 cm^{-1} was in good agreement with the O=Re=O stretches (range 780-850 cm^{-1}) for the Re(V) amine complexes reported by Engelbrecht et al.[9, 15] and showed the presence of the O=Re=O moiety.

The ^{1}H-NMR spectrum (Figure 3.4) of the complex left to crystallize at room temperature showed two isomers of the Re-products, whereas the ^{1}H-NMR spectrum (Figure 3.5) of the complex crystallized in the freezer showed only one isomer of the Re-product. This might be due to lower solubility of one conformation at the lower temperature, with the other conformation remaining in solution.

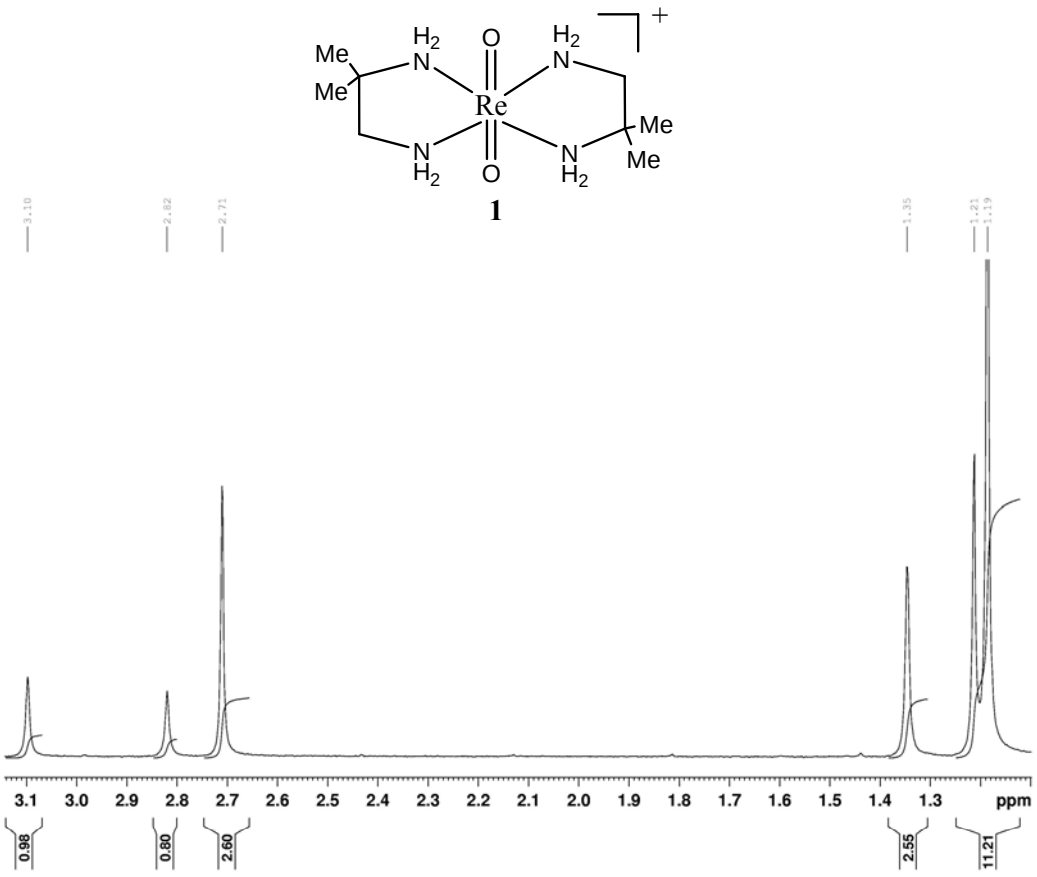

1

Figure 3.4: ^{1}H-NMR spectrum of $[ReO_2(H_2NCH_2C(CH_3)_2NH_2)_2](Cl)$ (1) in D_2O

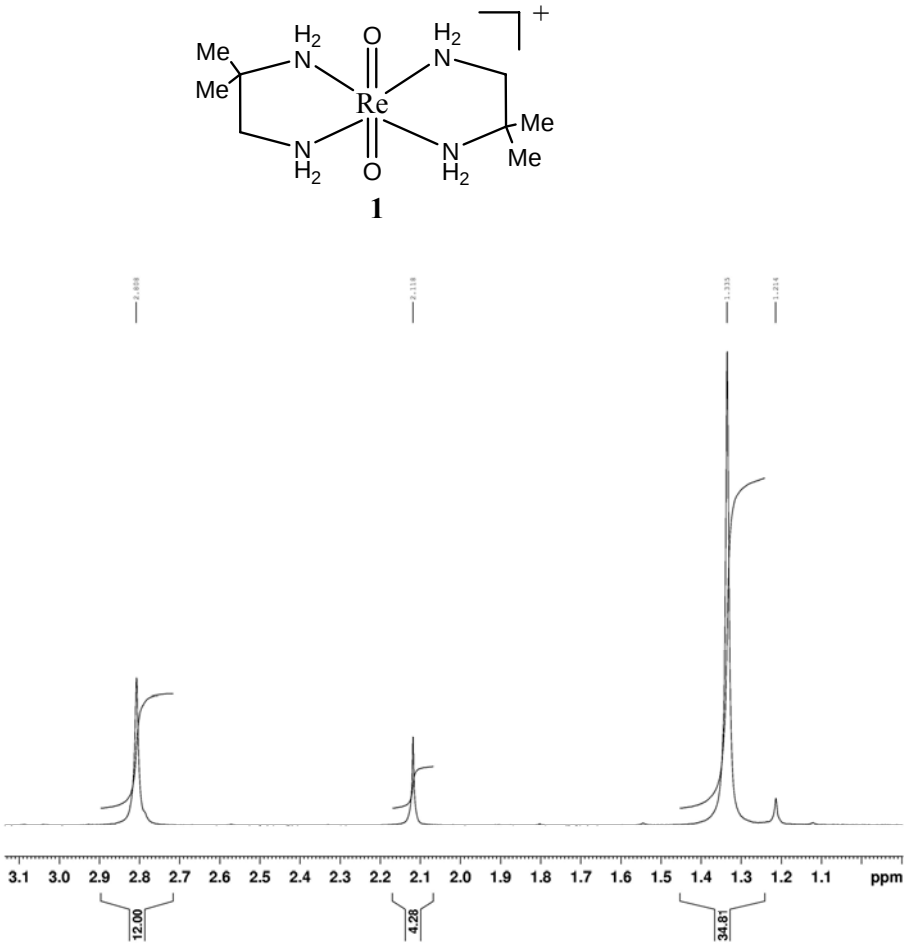

1

Figure 3.5: ^{1}H-NMR spectrum of refrigerated $[ReO_2(H_2NCH_2C(CH_3)_2NH_2)_2](Cl)$ (1) in D_2O

Complex **2** was synthesized by adding perchloric acid to complex **1.** Complex **2** formed pink colored crystals. Complex **2** was characterized by ^{1}H-NMR (Appendix A: Figure 3.8), IR and mass spectroscopies.

The IR stretch at 983 cm^{-1} was in good agreement with the Re=O stretches (range 900-1000 cm^{-1}) for Re(V) amine complexes reported by Engelbrecht et al.[9,15] and showed the presence of the Re=O group. The mass spectrum (Appendix A: Figure 3.9) shows an

m/z for the singly charged rhenium complex at 395. This is in good agreement with the calculated value (395.5) for the complex in the absence of the counter ion.

3.3.2 Synthesis of $[ReO(OH)(H_2N(CH_2)_2N(CH_3)_2)_2](CF_3SO_3)_2$ (4)

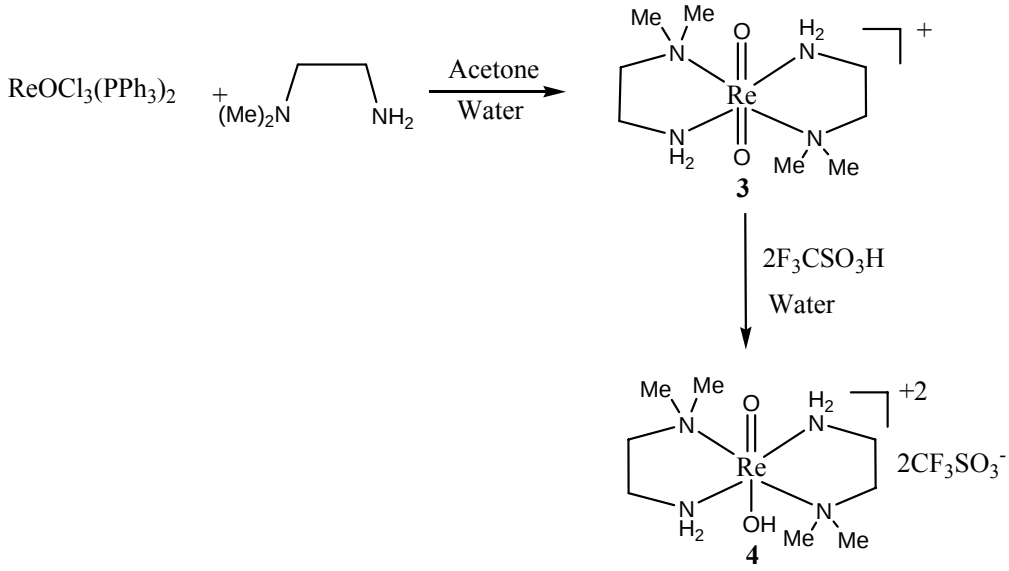

Scheme 3.2: Synthetic route for $[ReO(OH)(H_2N(CH_2)_2N(CH_3)_2)_2](CF_3SO_3)_2$ (4)

Complex **4** was also synthesized by modifying the synthetic route reported by Engelbrecht.[9] (Scheme 3.2). Excess N,N-dimethyl-ethylenediamine (40 fold) was used to obtain complex **3**. Complex **3** was characterized using ^{1}H-NMR (Appendix A: Figure 3.10) and IR spectroscopies. The IR stretch at 832 cm^{-1} was in good agreement with the O=Re=O stretches (range 780-850 cm^{-1}) for Re(V) amine complexes reported by Engelbrecht et al.[9, 15] and showed the presence of the O=Re=O moiety.

Complex **4** was synthesized by adding triflic acid to complex **3.** Complex **4** formed red colored crystals. Complex **4** was characterized by ^{1}H-NMR (Appendix A: Figure 3.11), IR and mass spectroscopies. The IR stretch at 976 cm^{-1} was in good agreement

with the Re=O stretches (range 900-1000 cm^{-1}) for Re(V) amine complexes reported by Engelbrecht et al.[9,15] and showed the presence of the Re=O group.

The mass spectrum (Appendix A: Figure 3.12) shows an m/z for the singly charged rhenium complex at 395. This is in good agreement with the calculated value (395.5) for the complex in the absence of the counter ion.

3.3.3 Determination of the Acid Dissociation Constants of $[ReO_2(H_2NCH_2C(CH_3)_2NH_2)_2]Cl$

The pKa_2 determination for the protonation of one oxo group in $[ReO_2(H_2NCH_2C(CH_3)_2NH_2)_2]^+$**(1)** to form $[ReO(OH)(H_2NCH_2C(CH_3)_2NH_2)_2]^{2+}$ **(2)** is illustrated in Figure 3.6, and the values obtained from the non-linear least square fit are summarized in Table 3.1.

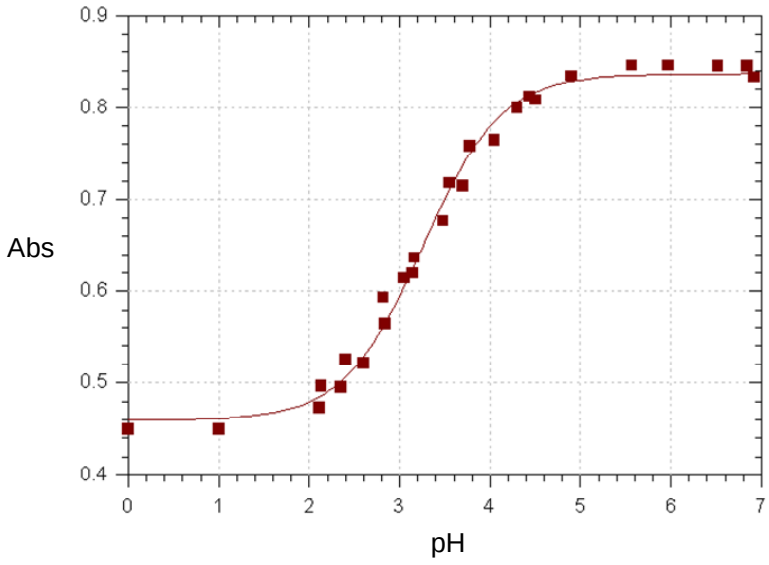

Figure 3.6: Plot of Absorbance. *vs.* pH for $[ReO_2(H_2NCH_2C(CH_3)_2NH_2)_2]^+$(1) at 25°C. [Re] = 2 x 10^{-3} M, μ = 1 M ($NaClO_4$), λ = 240 nm

3.3.4 Determination of the Acid Dissociation Constants of $[ReO_2(H_2N(CH_2)_2N(CH_3)_2)_2]Cl$ (3)

The pKa_2 determination for the protonation of one oxo group in $[ReO_2(H_2N(CH_2)_2N(CH_3)_2)_2]^+$**(3)** to form $ReO(OH)(H_2N(CH_2)_2N(CH_3)_2)_2]^{2+}$**(4)** is illustrated in Figure 3.7, and the values obtained from the non-linear least square fits are summarized in Table 3.1.

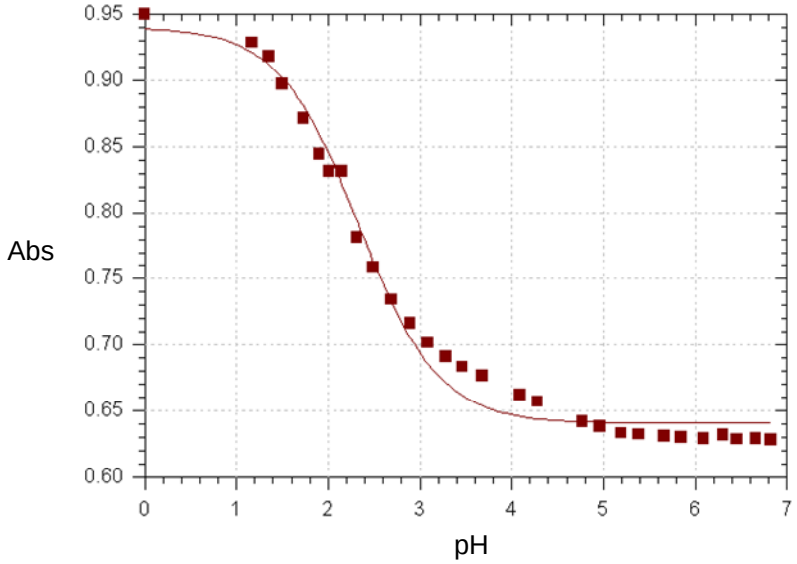

Figure 3.7: Plot of Absorbance. *vs.* pH for $[ReO_2(H_2N(CH_2)_2N(CH_3)_2)_2]^+$ (3) at 25°C. [Re] = 2 x 10^{-3} M, μ = 1 M ($NaClO_4$), λ = 240 nm

Determination of the pKa_2 values of complexes **1** and **3** was done and compared these values with other functionalized rhenium amine complexes which were reported in the literature (Table 3.1).[9,12-16]

Complex	pK_{a1}	pK_{a2}	References
$[ReO_2H_2N(CH_2)_2NH_2)_2]^+$	-0.9	3.26	12, 16
$[ReO_2(H_2NCH_2C(CH_3)_2NH_2)_2]^+$	--	**3.25**	**Our work**
$[ReO_2(HN(C_2H_5)(CH_2)_2NH_2)_2]^+$	--	2.77 (1)	9, 12
$[ReO_2(H_2N(CH_2)_2N(CH_3)_2)_2]^+$	--	**2.33**	**Our work**
$[ReO_2(HN(CH_3)(CH_2)_2(CH_3)NH)_2]^+$	-0.23	2.23 (1)	9, 13
$[ReO_2(N(C_2H_5)_2(CH_2)_2NH_2)_2]^+$	--	2.06 (2)	14, 15
$[ReO_2(N(CH_3)_2(CH_2)_2(CH_3)_2N)_2]^+$	--	0.32 (9)	9, 15

Table 3.1: Acid dissociation constants determined for $[ReO_2(EN)_2]^+$ type complexes

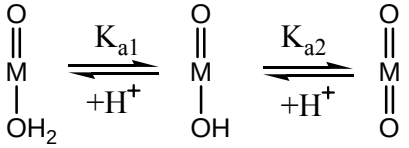

Scheme 3.3: Protonation of the *trans*-$[MO_2]^+$ Core

pKa1 = -log Ka_1 and pKa_2 = -log Ka_2, where Ka_1 and Ka_2 are acid dissociation constants. Lower pKa means lower basicity.

Functionalizing the ethylenediamine type ligands decreases the pKa values of the complexes rather than increasing them. For example, the unfunctionalized ethylenediamine complex $[ReO_2(H_2N(CH_2)_2NH_2)_2]^+$ has a pKa_2 value of 3.26, whereas pKa_2 values of functionalized amine nitrogen complexes listed in Table 3.1 were lower than 3.26. The lower pKa value indicates weaker Lewis base character with less electron density available on the nitrogen atoms for donation to the Re center. This might be due

to functionalization of the amine nitrogen, which may cause the structure to be sterically hindered. This may result in a more electron deficient rhenium center, thus the Re(V) may tend to accept π electrons from the oxo group, which results in stronger Re=O bonds that are more difficult to protonate. However functionalization of the carbon backbone did not change the pKa_2 value of the Re-amine complex much.

From our experiments we can conclude that the complex with N,N-dimethyl-ethylenediamine, in which there are two methyl groups on the nitrogen, and 1,2-diamino-2-methylpropane as the ligand, in which there are two methyl groups on the carbon backbone, further confirmed the observation of Engelbrecht.,[9] that functionalizing the ethylenediamine type ligands decreases the pKa values of the complexes rather than increasing them.

3.3.5 Synthesis of trans-$[ReCl(PEt_3)(S(CH_2)_2NH_2)_2]$ (6)

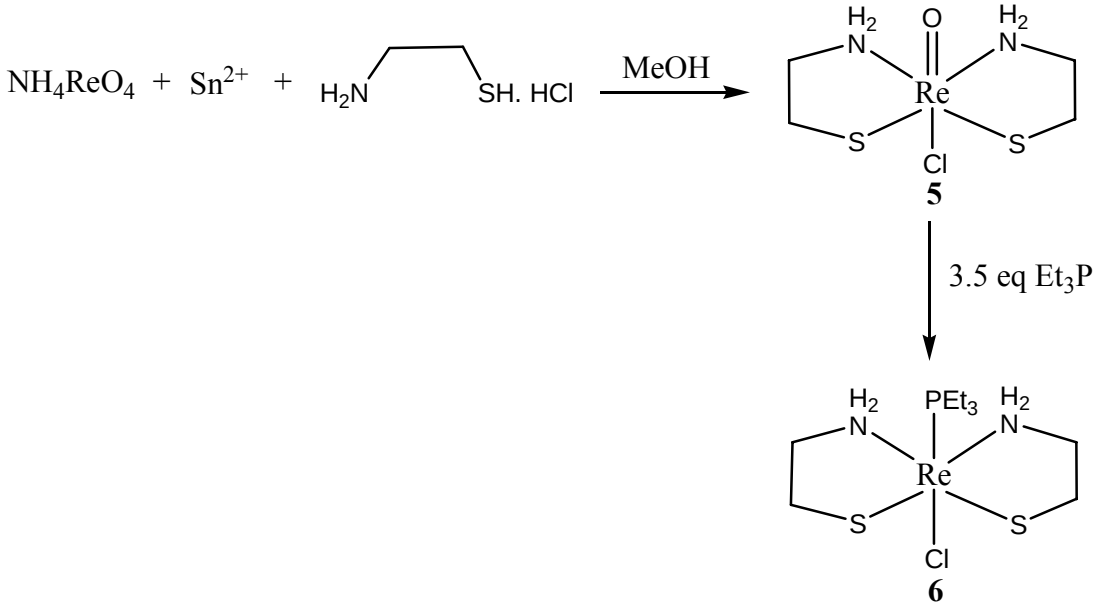

Scheme 3.4: Synthetic route for trans-$[Re^{III}Cl(PEt_3)(S(CH_2)_2NH_2)_2]$ (6)

Complex **5** was synthesized following the synthetic route used by Takumi et al.,[10] and was characterized by ^{1}H-NMR (Appendix A: Figure 3.13) and IR spectroscopies.

Complex **6** was synthesized by adding excess triethylphosphine (3.5 equivalents) to complex **5**. Complex **6** was characterized by ^{1}H-NMR (Appendix A: Figure 3.14), ^{31}P-NMR (Appendix A: Figure 3.15), IR and mass spectroscopies (Appendix A: Figure 3.16). The mass spectrum shows an m/z for the singly charged rhenium complex at 493. This is in good agreement with the calculated value (493.10) for the complex.

The solubility of the product was very poor. It was soluble only in very polar solvents like water but not in any of the other solvents tested. Because of this reason we could not further study this complex. If the solubility of the product was good we would have tried to crystallize the product. We would also have extended this work to make tetradentate rhenium(III) complexes.

3.4 Conclusions

This chapter describes the synthesis and characterization of three rhenium complexes, two of them with ethylenediamine type ligands in which the rhenium is in +5 oxidation state and the third complex with the 2-aminoethanethiolate ligand and a phosphine ligand in which the rhenium is in the +3 oxidation state.

The presence of the oxo group in each complex was confirmed by IR spectroscopy. The NMR spectra confirmed the formation of the final product in each case. Mass spectrometry further confirmed the formation of the desired products by showing the expected molecular ion for each complex.

The acid dissociation constants (pKa_2 values) for the co-ordinated oxo groups showed that the Re-complex with the 1,2-diamino-2-methylpropane is more basic than the complex with N,N-dimethyl ethylenediamine. When comparing functionalized ethylenediamine type ligands with unfunctionalized ones, the functionalized

ethylenediamine type ligands resulted in lower pKa values for the complexes. This further supports the observation that by the functionalization of ethylenediamine type ligands decreased the pKa values of the oxo group of the Re(V) complexes rather than increasing them.

3.5 Experimental

3.5.1 General Considerations.

Unless noted, all common laboratory chemicals were of reagent grade or better. Solvents were degassed with nitrogen prior to use, and all experiments were carried out under a nitrogen atmosphere. ^{1}H-NMR spectra were recorded in deuterium oxide on a Bruker 250 MHz instrument at 25˚C. FT-IR spectra were obtained as KBr pellets on a Nicolet Magna-IR spectrometer 550. UV-VIS spectra were recorded on a Hewlet Packard 8452 diode array spectrophotometer.

3.5.2 $[ReO_2(H_2NCH_2C(CH_3)_2NH_2)_2]Cl$ (1)

$[ReOCl_3(PPh_3)_2]$ (250 mg, 0.3 mmol) was suspended in a mixture of acetone (20 mL) and water (0.6 mL). To this suspension, 1,2-diamino-2-methylpropane {Re: en, 1:~40} was added while stirring. The mixture was refluxed for 90 min under nitrogen atmosphere and allowed to cool. The precipitate was collected by filtration, washed with toluene and ether, and dried overnight in a vacuum desiccator over P_2O_5. The yellowish brown product was divided into two parts. The first part was left at room temperature. (Yield: 80 mg, 70%) Spectral data: **IR** [KBr, ν in cm^{-1}]: 821 (O=Re=O). ^{1}H **NMR** [D_2O, 250 MHz; δ (ppm)]: 2.71 (H_2N-**CH_2**-$C(CH_3)_2NH_2$, s, 4H); 2.82 (H_2N-**CH_2**-$C(CH_3)_2NH_2$, s, 4H); 1.19 (H_2N-CH_2-C**$(CH_3)_2$**NH_2, s, 12H); 1.36 (H_2N-CH_2-C**$(CH_3)_2$**NH_2, s, 12H).

The second part was left in the freezer. Spectral data: **IR** [KBr, ν in cm^{-1}]: 825 (O=Re=O). ^{1}H **NMR** [D_2O, 250 MHz; δ (ppm)]: 2.80 (H_2N-**CH_2**-$C(CH_3)_2NH_2$, s, 4H); 1.33 (H_2N-CH_2-C**$(CH_3)_2$**NH_2, s, 12H).

3.5.3 $[ReO(OH)(H_2NCH_2C(CH_3)_2NH_2)_2](ClO_4)_2$ (2)

$HClO_4$ (10 drops) was added to 25 mg of $[ReO_2(H_2NCH_2C(CH_3)_2NH_2)_2]Cl$ **(1)** in 2 mL of water. The resulting pink crystals were collected after a day of slow evaporation of the solvent. (Yield: 20 mg, 60%) Spectral data: **IR** [KBr, ν in cm^{-1}], 983 (Re=O). ^{1}H **NMR** [D_2O, 250 MHz; δ (ppm)]: 2.90 (H_2N-**CH_2**-$C(CH_3)_2$, s, 4H); 1.37 (H_2N-CH_2-C**$(CH_3)_2$**), s,12H). **MS** (*m/z*): $[M+H]^+$ 395; Calcd 395.5.

3.5.4 $[ReO_2(H_2N(CH_2)_2N(CH_3)_2)_2]Cl$ (3)

$[ReOCl_3(PPh_3)_2]$ (250 mg, 0.3 mmol) was suspended in a mixture of acetone (20 mL) and water (0.6 mL). To this suspension, N,N-dimethyl-ethylenediamine {Re: en, 1:~40} was added while stirring. The mixture was refluxed for 90 min under nitrogen atmosphere and allowed to cool, followed by filtration. The orange brown precipitate was washed with toluene (2 x 5 mL) and ether (2 x 5 mL) and dried overnight in a vacuum desiccator over P_2O_5. (Yield: 115 mg, 61%) Spectral data: **IR** [KBr pellet, ν in cm^{-1}]: 832 (O=Re=O). **^{1}H NMR** [D_2O, 250 MHz; δ (ppm)]: 2.55, 2.80 (H_2N-CH_2-CH_2-N**$(CH_3)_2$**), 2s, 12H,); 2.80-2.90 (H_2N-**CH_2-CH_2**-$N(CH_3)_2$, m, 4H); 2.60 (H_2N-CH_2-**CH_2**-$N(CH_3)_2$, t, 2H); 3.20 (H_2N-**CH_2**-CH_2-$N(CH_3)_2$, t, 2H).

3.5.5 $[ReO(OH)(NH_2(CH_2)_2N(CH_3)_2)_2](CF_3SO_3)_2$ (4)

This complex was obtained by dissolving $[ReO_2(NH_2(CH_2)_2N(Me)_2)_2]Cl$ **(3)** (25 mg) in 2 mL of water and adding 10 drops of CF_3SO_3H. The resulting red crystals were collected after 3 days of slow evaporation of the solvent. (Yield: 25 mg, 59%) Spectral data: **IR** [KBr, ν in cm^{-1}] 1037.3 (Re=**O**). **^{1}H NMR** [D_2O, 250 MHz, δ (ppm)]: 2.85 (H_2N-CH_2-**CH_2**-$N(CH_3)_2$, t, 4H); 3.10 (H_2N-**CH_2**-CH_2-$N(CH_3)_2$, t, 4H); 2.87 (H_2N-CH_2-CH_2-N-**$(CH_3)_2$**, s, 12H). **MS** (*m/z*): $[M+H]^+$ 395; calcd 395.5.

3.5.6 Determination of the Acid Dissociation Constants of $[ReO_2(EN)_2]^+$ Type Complexes

A solution of the Re-complex (0.002 M) was prepared in 1 M $NaClO_4$ (10 mL). The pH meter was calibrated with pH 7 buffer and then with pH 4 buffer. The absorbance of the blank (1 M $NaClO_4$) was determined, followed by the absorbance of the complex (0.002 M Rhenium complex + $NaClO_4$). Perchloric acid (20%) was added slowly in 0.2mL to 0.3mL increments and the pH and absorbance values were noted until pH 2 was reached. The pKa values were determined using the SCIENTIST [11] fitting program and by using non-linear least squares fit.

3.5.7 $[Re^{III}Cl(PEt_3)(S(CH_2)_2NH_2)_2]$ (6)

$[Re^{V}O(Cl)(S(CH_2)_2NH_2)_2]$ **(5)** was prepared using the procedure by Takumi et al.[11] Complex **(6)** was synthesized by adding triethylphosphine (0.34 mL, 4.5 mmol) to 10 mL of a methanol solution of $[Re^{V}O(Cl)(S(CH_2)_2NH_2)_2]$ (0.5 g, 1.3 mmol). The mixture was refluxed overnight under a nitrogen atmosphere, allowed to cool. The brownish black solution was dried and characterized. (Yield: 400 mg, 48%) Spectral data: **^{1}H NMR**

[D_2O, 250 MHz, δ (ppm)]: 1.73-1.81 ((CH_3-**CH_2)$_3$-**P, m, 6H); 1.00-1.13 (**(CH_3-**CH_2)-P, m, 9H); 2.94-3.00 (NH_2-CH_2**CH_2-**S, 2t, 8H); 3.35 (NH_2**CH_2**CH_2S, t, 4H); **MS** (*m/z*): $[M+H]^+$ 493.02; calcd 493.10.

References

1. Treichel, P. M. *Kirk-Othmer Encyclopaedia of Chemical Technology (*3rd Ed.), **20,** John Wiley and Sons, New York, **1982**.

2. Mathews, C. K.; Van Holde, K. E.; Biochemistry, Benjamin/Cummings Publishing Company, Inc., Redwood City, **1990**.

3. Bandoli, G.; Dolmella, A.; Gerber, T.I.A.; Perils, J.; du Preez, J. G. H. The Reaction of nitro 1,2-diaminobenzenes with $[ReO]^{3+}$ core: isolation of oxo-free rhenium(V) complexes. *Inorg. Chim. Acta*. **2000**, 303, 24-29.

4. Marchi, A.; Garuti, P.; Duatti, A.; Magon, L.; Bertolasi, V. Synthesis of technetium(V)-nitrido complexes with chelating amines: a novel class of monocationic, octahedral complexes containing the $[Tc.tplbond.N]^{2+}$ core. Crystal structures of $[TcN(en)_2Cl]^{+}$ (en = ethylenediamine) and [TcN(tad)Cl]+ (tad = 1,5,8,12,-tetraazadodecane). *Inorg. Chem*. **1990,** 29, 2091-2096.

5. Parker, D.; Roy, P. S. Synthesis and characterization of stable rhenium(V) dioxo complexes with acyclic tetraamine ligands, $[LReO_2]^{+}$. *Inorg. Chem*. **1988,** 27, 4127-4130.

6. Zuckman, S. A.; Freeman, G. M.; Troutner, D. E.; Volkert W. A.; Holmes, R. A.; Van Derveer, D. G.; Barefield, E. K. Preparation and X-ray structure of trans-dioxo(1,4,8,11-tetraazaxyclotetradecane)technetium(V) perchlorate hydrate. *Inorg. Chem*. **1981**, 20, 2386-2389.

7. Jurisson S. S.; Aston, K.; Faor, C. K.; Schlemper, E. O.; Sharp, P. R.; Troutner, D. E. Effect of ring size on properties of technetium amine complexes. X-ray structures of $TcO_2Pent(AO)_2$, which contains an unusual eight-membered chelate ring, and of $TcOEn(AO)_2$. *Inorg. Chem*. **1987**, 26, 3576-3582.

8. Jurisson, S. S.; Berning, D.; Jia, W.; Ma, D. Coordination compounds in nuclear medicine. *Chem Rev.* **1993,** 93, 1137-1156.

9. Engelbrecht, H.P., Ph D thesis. **2001**.

10. Takumi, K.; Yuichi, S.; Masayuki, K.; Masakazu, H. Synthesis, Characterization, and Stereochemistry of oxorhenium(V) Complexes with 2-Aminoethanethiolate. *Inorg Chem*. **2001,** 40, 4250-4256.

11. MicroMath Scientist Software for Windows.

12. Basolo, F.; Murmann, R.K Dissociation constants of N-alkylethylenediamines. *J. Am. Chem. Soc.* 1952, 74, 2373-2374.

13. Gustafson, R. L.; Martell, A. E. Hydrolytic tendencies of metal chelate compounds. V. Hydrolysis and dimerization of copper (II) chelates with 1,2-diamines. *J. Am. Chem. Soc.* **1959,** 81, 525-529.

14. Irving, H. M.; Griffiths, J. M. M. The stabilities of complexes formed by some bivalent transition metals with N-alkyl-substituted ethylenediamines. *J. Chem. Soc.* **1954.** 213-223.

15. Engelbrecht, H. P.; Otto, S.; Roodt, A. trans-Bis(N,N-diethylenediamine-N,N')dioxorhenium(V) chloride trihydrate. Acta Crystallogr. Sect. C. 199, C55, 1648-1650.

16. Basolo, F.; Murmann, R. K. Steric effects and the stability of complex compounds. I. The chelating tendencies of N-alkylethylenediamines, with copper(II) and nickel(II) ion. *J. Am. Chem. Soc.* 1952, 74, 5243-5246.

APPENDIX-A

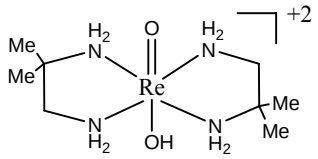

2

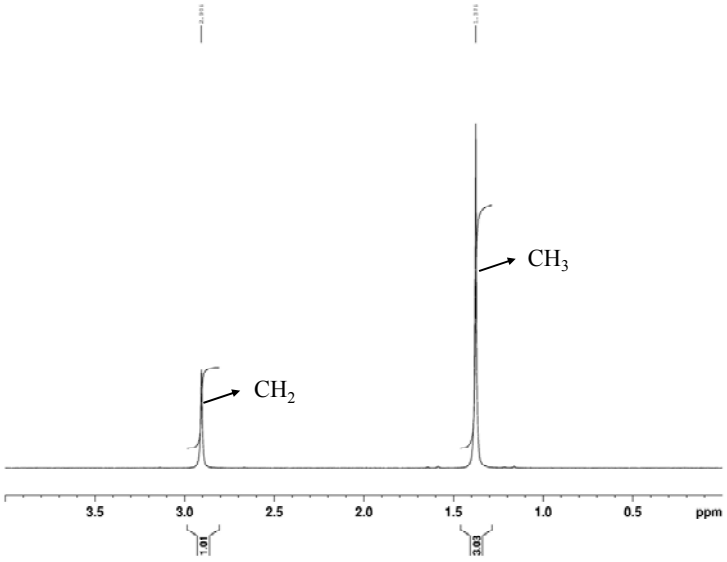

Figure 3.8: ^{1}H-NMR spectrum of $[ReO(OH)(H_2NCH_2C(CH_3)_2NH_2)_2](ClO_4)_2$ (2) in D_2O

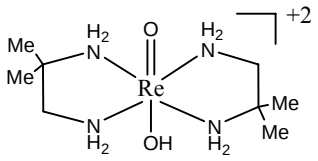

2

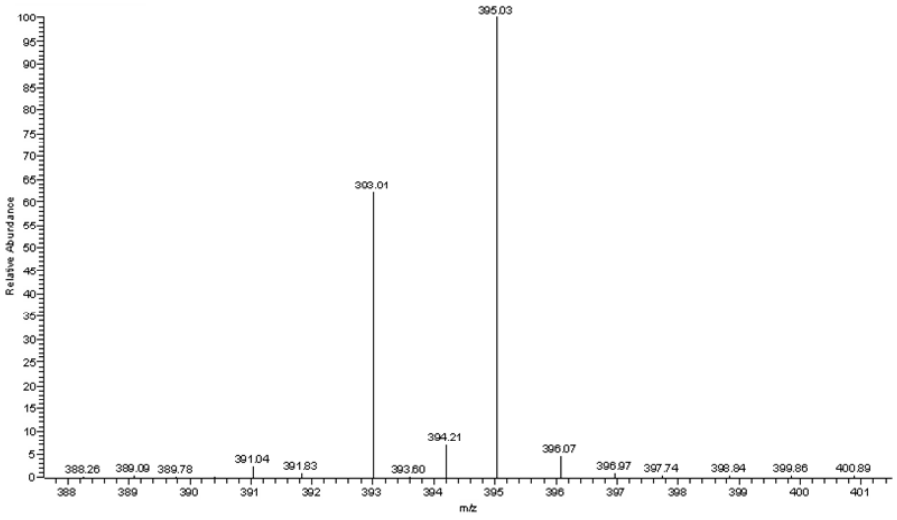

Figure 3.9: ESI-MS Spectrum of $[ReO(OH)(H_2NCH_2C(CH_3)_2NH_2)_2]^{2+}$ (2)

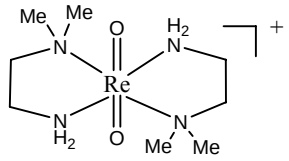

3

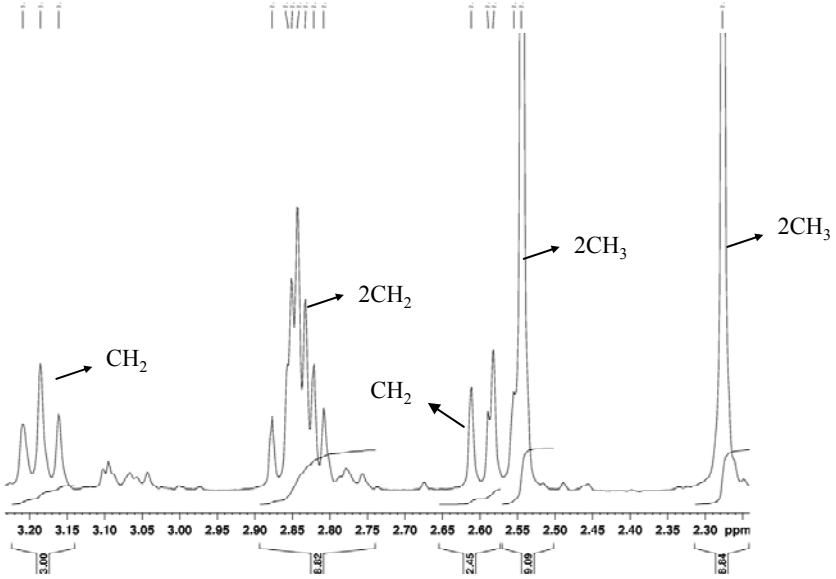

Figure 3.10: ^{1}H NMR spectrum of $[ReO_2(H_2N(CH_2)_2N(CH_3)_2)_2](Cl)$ in D_2O (3)

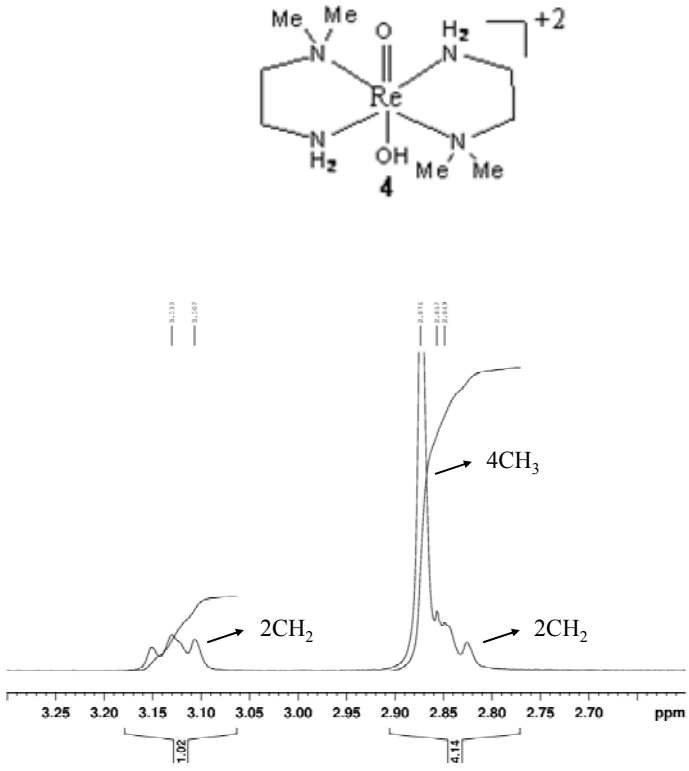

Figure 3.11: ^{1}H NMR spectrum of $[ReO(OH)(H_2N(CH_2)_2N(CH_3)_2)_2](CF_3SO_3)_2$ in D_2O

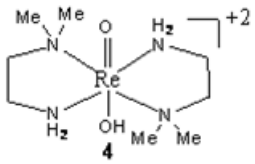

4

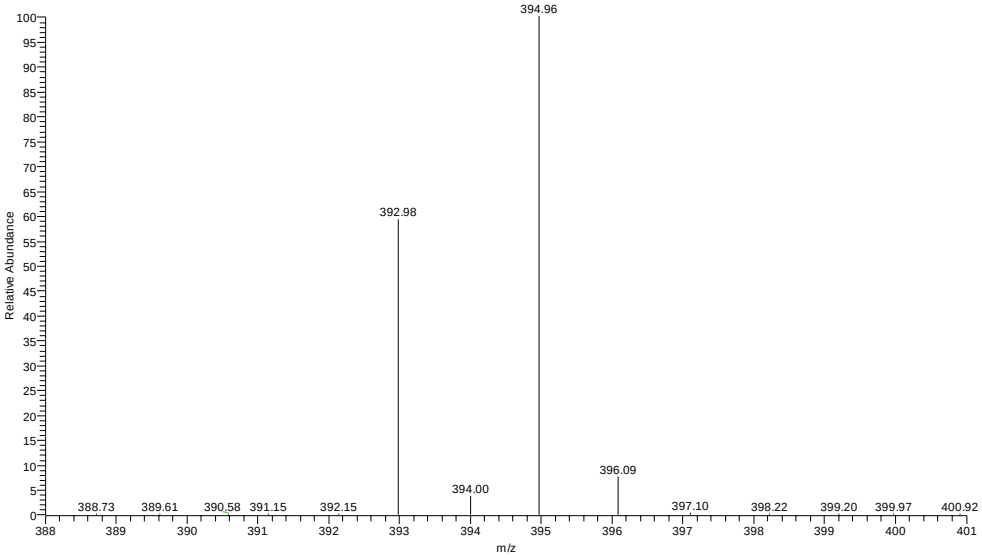

Figure 3.12: ESI-MS spectrum of $[ReO(OH)(H_2N(CH_2)_2N(CH_3)_2)_2]^{2+}$

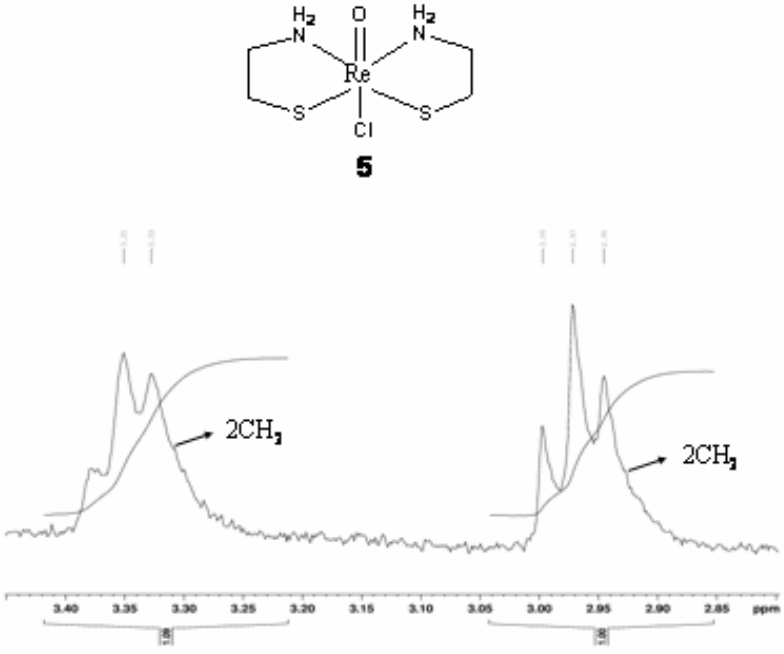

Figure 3.13: ^{1}H NMR spectrum of $[Re^{V}O(Cl)(S(CH_2)_2NH_2)_2]$ in D_2O

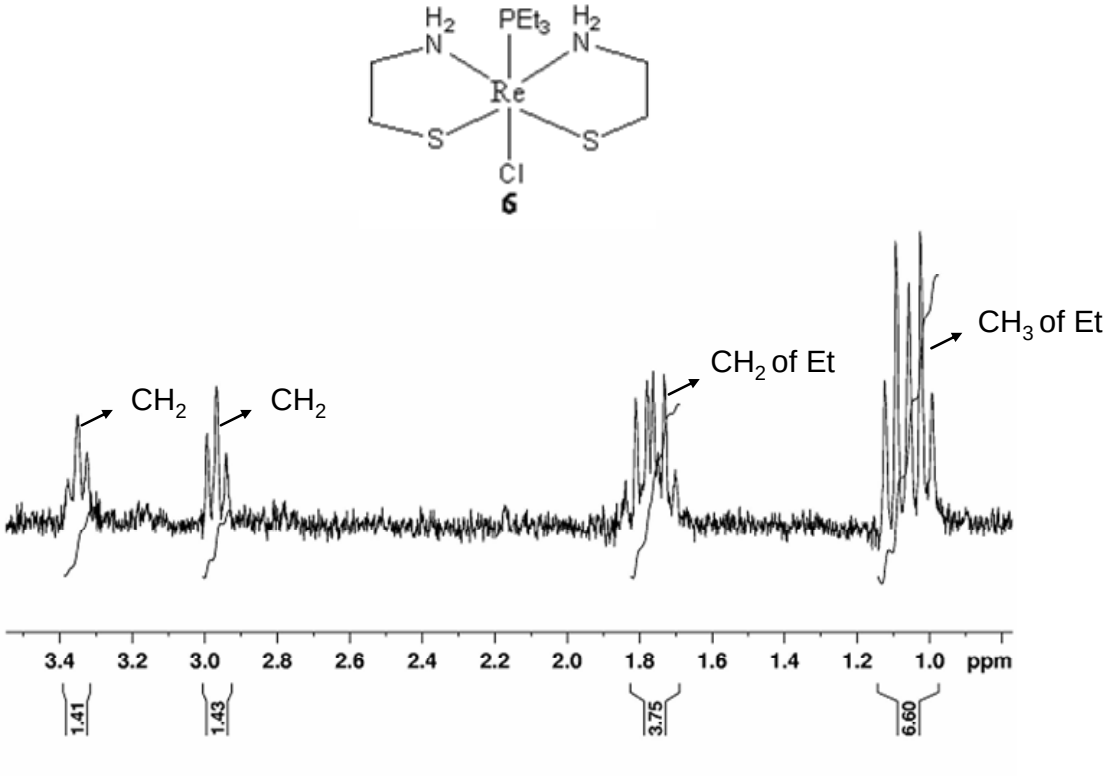

Figure 3.14: ^{1}H NMR spectrum of [Re^{III}Cl (PEt_3)($S(CH_2)_2NH_2)_2$] (6) in D_2O

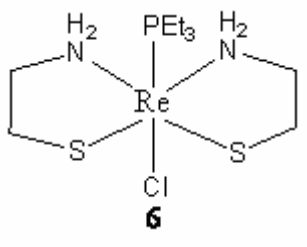

6

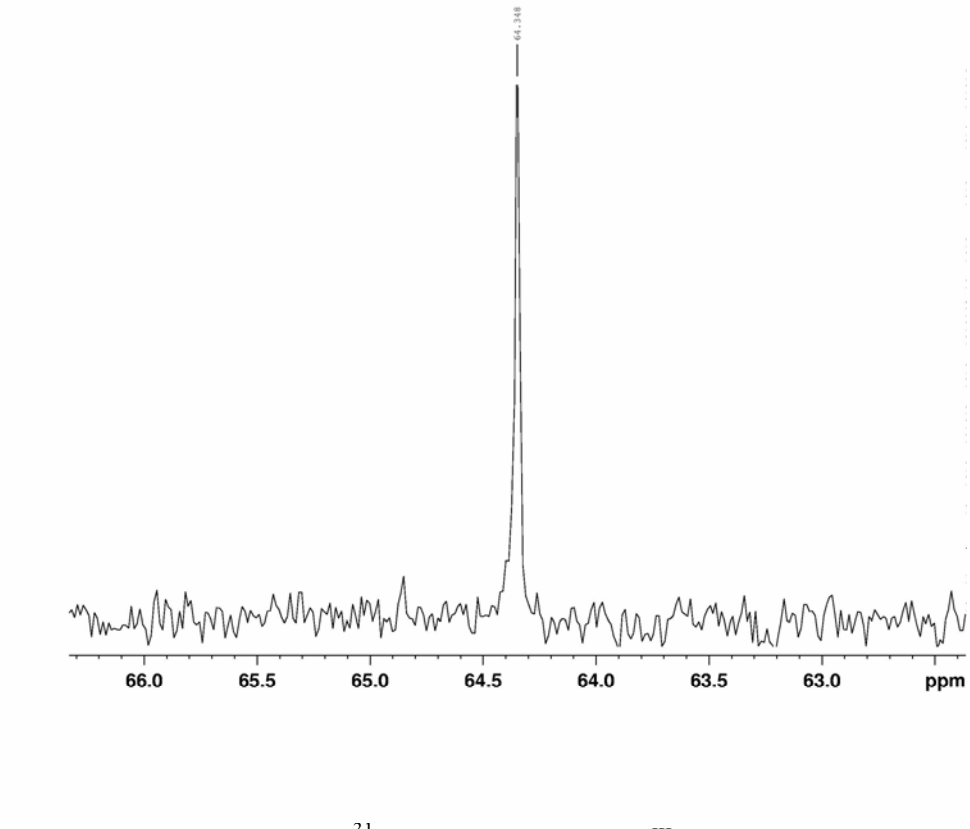

Figure 3.15: ^{31}P-NMR spectrum of [$Re^{III}Cl(PEt_3)(S(CH_2)_2NH_2)_2$]

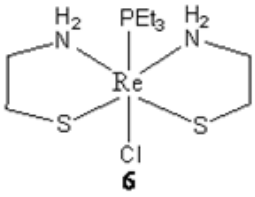

6

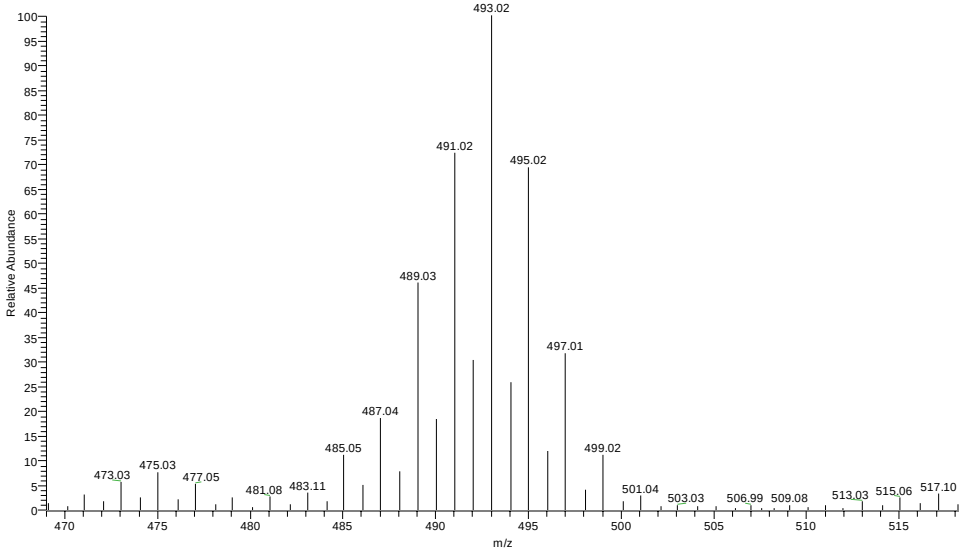

Figure 3.16: ESI-MS spectrum of [$Re^{III}Cl(PEt_3)(S(CH_2)_2NH_2)_2$]

VITA

Sulochana Junnotula was born to Bobbala Raji Reddy and Pushpa Latha on June 23rd in Mallanna Palle, Andhra Pradesh, India. She has a brother (Ravinder Reddy) and a sister (Manjula). After her high school in Huzurabad she went to Srichaithanya Mahila Kalasala to study intermediate education. She has done her B.Pharm in Rajiv Gandhi University of Health Sciences. She is married to Venkatraman Junnotula on June 19th 2002. She continued her education at University of Missouri Columbia, Department of Chemistry, earning her M.S. in 2006.